Advances in Adaptive Data Analysis
Vol. 1, No. 1 (2009) 1–41

World Scientific
www.worldscientific.com

ENSEMBLE EMPIRICAL MODE DECOMPOSITION: A NOISE-ASSISTED DATA ANALYSIS METHOD

ZHAOHUA WU* and NORDEN E. HUANG†

*Center for Ocean–Land–Atmosphere Studies
4041 Powder Mill Road, Suite 302
Calverton, MD 20705, USA

†Research Center for Adaptive Data Analysis
National Central University
300 Jhongda Road, Chungli, Taiwan 32001

A new Ensemble Empirical Mode Decomposition (EEMD) is presented. This new approach consists of sifting an ensemble of white noise-added signal (data) and treats the mean as the final true result. Finite, not infinitesimal, amplitude white noise is necessary to force the ensemble to exhaust all possible solutions in the sifting process, thus making the different scale signals to collate in the proper intrinsic mode functions (IMF) dictated by the dyadic filter banks. As EEMD is a time–space analysis method, the added white noise is averaged out with sufficient number of trials; the only persistent part that survives the averaging process is the component of the signal (original data), which is then treated as the true and more physical meaningful answer. The effect of the added white noise is to provide a uniform reference frame in the time–frequency space; therefore, the added noise collates the portion of the signal of comparable scale in one IMF. With this ensemble mean, one can separate scales naturally without any *a priori* subjective criterion selection as in the intermittence test for the original EMD algorithm. This new approach utilizes the full advantage of the statistical characteristics of white noise to perturb the signal in its true solution neighborhood, and to cancel itself out after serving its purpose; therefore, it represents a substantial improvement over the original EMD and is a truly noise-assisted data analysis (NADA) method.

Keywords: Empirical Mode Decomposition (EMD); ensemble empirical mode decompositions; noise-assisted data analysis (NADA); Intrinsic Mode Function (IMF); shifting stoppage criteria; end effect reduction.

1. Introduction

The Empirical Mode Decomposition (EMD) has been proposed recently[1,2] as an adaptive time–frequency data analysis method. It has been proved quite versatile in a broad range of applications for extracting signals from data generated in noisy nonlinear and nonstationary processes (see, e.g., Refs. 3 and 4). As useful as EMD proved to be, it still leaves some annoying difficulties unresolved.

One of the major drawbacks of the original EMD is the frequent appearance of mode mixing, which is defined as a single Intrinsic Mode Function (IMF) either

consisting of signals of widely disparate scales, or a signal of a similar scale residing in different IMF components. Mode mixing is often a consequence of signal intermittency. As discussed by Huang *et al.*,[1,2] the intermittence could not only cause serious aliasing in the time–frequency distribution, but also make the physical meaning of individual IMF unclear. To alleviate this drawback, Huang *et al.*[2] proposed the intermittence test, which can indeed ameliorate some of the difficulties. However, the approach has its own problems: first, the intermittence test is based on a subjectively selected scale. With this subjective intervention, the EMD ceases to be totally adaptive. Second, the subjective selection of scales works if there are clearly separable and definable timescales in the data. In case the scales are not clearly separable but mixed over a range continuously, as in the case of the majority of natural or man-made signals, the intermittence test algorithm with subjectively defined timescales often does not work very well.

To overcome the scale separation problem without introducing a subjective intermittence test, a new noise-assisted data analysis (NADA) method is proposed, the Ensemble EMD (EEMD), which defines the true IMF components as the mean of an ensemble of trials, each consisting of the signal plus a white noise of finite amplitude. It should be noted here that we use word 'single' instead of word 'data' in this paper (except in some part of Sec. 2) because the purpose of this paper is to decompose the whole targeted data but not to identify the particular part that is known *a priori* as containing interesting information. Since there is added noise in the decomposition method, we refer the original data as 'signal' in most occasions. With this ensemble approach, we can clearly separate the scale naturally without any *a priori* subjective criterion selection. This new approach is based on the insight gleaned from recent studies of the statistical properties of white noise,[5,6] which showed that the EMD is effectively an adaptive dyadic filter bank[a] when applied to white noise. More critically, the new approach is inspired by the noise-added analyses initiated by Flandrin *et al.*[7] and Gledhill.[8] Their results demonstrated that noise could help data analysis in the EMD.

The principle of the EEMD is simple: the added white noise would populate the whole time–frequency space uniformly with the constituting components of different scales. When signal is added to this uniformly distributed white background, the bits of signal of different scales are automatically projected onto proper scales of reference established by the white noise in the background. Of course, each individual trial may produce very noisy results, for each of the noise-added decompositions consists of the signal and the added white noise. Since the noise in each trial is different in separate trials, it is canceled out in the ensemble mean of

[a]A dyadic filter bank is a collection of band-pass filters that have a constant band-pass shape (e.g., a Gaussian distribution) but with neighboring filters covering half or double of the frequency range of any single filter in the bank. The frequency ranges of the filters can be overlapped. For example, a simple dyadic filter bank can include filters covering frequency windows such as 50 to 120 Hz, 100 to 240 Hz, 200 to 480 Hz, etc.

enough trials. The ensemble mean is treated as the true answer, for, in the end, the only persistent part is the signal as more and more trials are added in the ensemble.

The critical concept advanced here is based on the following observations:

1. A collection of white noise cancels each other out in a time–space ensemble mean; therefore, only the signal can survive and persist in the final noise-added signal ensemble mean.
2. Finite, not infinitesimal, amplitude white noise is necessary to force the ensemble to exhaust all possible solutions; the finite magnitude noise makes the different scale signals reside in the corresponding IMF, dictated by the dyadic filter banks, and render the resulting ensemble mean more meaningful.
3. The true and physically meaningful answer to the EMD is not the one without noise; it is designated to be the ensemble mean of a large number of trials consisting of the noise-added signal.

This EEMD proposed here has utilized many important statistical characteristics of noise. We will show that *the EEMD utilizes the scale separation capability of the EMD, and enables the EMD method to be a truly dyadic filter bank for any data. By adding finite noise, the EEMD eliminated largely the mode mixing problem and preserve physical uniqueness of decomposition. Therefore, the EEMD represents a major improvement of the EMD method.*

In the following sections, a systematic exploration of the relation between noise and signal in data will be presented. Studies of Flandrin *et al.*[5] and Wu and Huang[6] have revealed that the EMD serves as a dyadic filter for various types of noise. This implies that a signal of a similar scale in a noisy data set could possibly be contained in one IMF component. It will be shown that adding noise with finite rather than infinitesimal amplitude to data indeed creates such a noisy data set; therefore, the added noise, having filled all the scale space uniformly, can help to eliminate the annoying mode mixing problem first noticed by Huang *et al.*[2] Based on these results, we will propose formally the concepts of NADA and noise-assisted signal extraction (NASE), and will develop a method called the EEMD, which is based on the original EMD method, to make NADA and NASE possible.

The paper is arranged as follows. Section 2 will summarize previous attempts of using noise as a tool in data analysis. Section 3 will introduce the EEMD method, illustrate more details of the drawbacks associated with mode mixing, present concepts of NADA and of NASE, and introduce the EEMD in detail. Section 4 will display the usefulness and capability of the EEMD through examples. Section 5 will further discuss the related issues to the EEMD, its drawbacks, and their corresponding solutions. A summary and discussion will be presented in the final section of the main text. Two appendices will discuss some related issues of EMD algorithm and a Matlab EMD/EEMD software for research community to use.

2. A Brief Survey of Noise-Assisted Data Analysis

The word "noise" can be traced etymologically back to its Latin root of "nausea," meaning "seasickness." Only in Middle English and Old French does it start to gain the meaning of "noisy strife and quarrel," indicating something not at all desirable. Today, the definition of noise varies in different circumstances. In science and engineering, noise is defined as disturbance, especially a random and persistent kind that obscures or reduces the clarity of a signal. In natural phenomena, noise could be induced by the process itself, such as local and intermittent instabilities, irresolvable subgrid phenomena, or some concurrent processes in the environment in which the investigations are conducted. It could also be generated by the sensors and recording systems when observations are made. When efforts are made to understand data, important differences must be considered between the clean signals that are the direct results of the underlying fundamental physical processes of our interest ("the truth") and the noise induced by various other processes that somehow must be removed. In general, all data are amalgamations of signal and noise, i.e.,

$$x(t) = s(t) + n(t), \tag{1}$$

in which $x(t)$ is the recorded data, and $s(t)$ and $n(t)$ are the true signal and noise, respectively. Because noise is ubiquitous and represents a highly undesirable and dreaded part of any data, many data analysis methods were designed specifically to remove the noise and extract the true signals in data, although often not successful.

Since separating the signal and the noise in data is necessary, three important issues should be addressed: (1) The dependence of the results on the analysis methods used and assumptions made on the data. (For example, a linear regression of data implicitly assumes the underlying physics of the data to be linear, while a spectrum analysis of data implies the process is stationary.) (2) The noise level to be tolerated in the extracted "signals," for no analysis method is perfect, and in almost all cases the extracted "signals" still contain some noise. (3) The portion of real signal obliterated or deformed through the analysis processing as part of the noise. (For example, Fourier filtering can remove harmonics through low-pass filtering and thus deform the waveform of the fundamentals.)

All these problems cause misinterpretation of data, and the latter two issues are specifically related to the existence and removal of noise. As noise is ubiquitous, steps must be taken to insure that any meaningful result from the analysis should not be contaminated by noise. To avoid possible illusion, the null hypothesis test against noise is often used with the known noise characteristics associated with the analysis method.[6,9,7] Although most data analysis techniques are designed specifically to remove noise, there are, however, cases when noise is added in order to help data analysis, to assist the detection of weak signals, and to delineate the underlying processes. The intention here is to provide a brief survey of the beneficial utilization of noise in data analysis.

The earliest known utilization of noise in aiding data analysis was due to Press and Tukey[10] known as pre-whitening, where white noise was added to flatten the narrow spectral peaks in order to get a better spectral estimation. Since then, pre-whitening has become a very common technique in data analysis. For example, Fuenzalida and Rosenbluth[11] added noise to process climate data; Link and Buckley,[12] and Zala *et al.*[13] used noise to improve acoustic signal; Strickland and Il Hahn[14] used wavelet and added noise to detect objects in general; and Trucco[15] used noise to help design special filters for detecting embedded objects on the ocean floor experimentally. Some general problems associated with this approach can be found in the works by Priestley,[16] Kao *et al.*,[17] Politis,[18] and Douglas *et al.*[19]

Another category of popular use of noise in data analysis is more related to the analysis method than to help extracting the signal from the data. Adding noise to data helps to understand the sensitivity of an analysis method to noise and the robustness of the results obtained. This approach is used widely; for example, Cichocki and Amari[20] added noise to various data to test the robustness of the independent component analysis (ICA) algorithm, and De Lathauwer *et al.*[21] used noise to identify error in ICA.

Adding noise to the input to specifically designed nonlinear detectors could also be beneficial to detecting weak periodic or quasi-periodic signals based on a physical process called stochastic resonance. The study of stochastic resonance was pioneered by Benzi and his colleagues in the early 1980s. The details of the development of the theory of stochastic resonance and its applications can be found in a lengthy review paper by Gammaitoni *et al.*[22] It should be noted here that *most of the past applications (including those mentioned earlier) have not used the cancellation effects associated with an ensemble of noise-added cases to improve their results.*

Specific to analysis using EMD, Huang *et al.*[23] added infinitesimal magnitude noise to earthquake data in an attempt to prevent the low frequency mode from expanding into the quiescent region. But they failed to realize fully the implications of the added noise in the EMD method. The true advances related to the EMD method had to wait until the two pioneering works by Gledhill[8] and Flandrin *et al.*[7]

Flandrin *et al.*[7] used added noise to overcome one of the difficulties of the original EMD method. As the EMD is solely based on the existence of extrema (either in amplitude or in curvature), the method ceases to work if the data lacks the necessary extrema. An extreme example is in the decomposition of a Dirac pulse (delta function), where there is only one extrema in the whole data set. To overcome the difficulty, Flandrin *et al.*[7] suggested adding noise with infinitesimal amplitude to the Dirac pulse so as to make the EMD algorithm operable. Since the decomposition results are sensitive to the added noise, Flandrin *et al.*[7] ran an ensemble of 5000 decompositions, with different realizations of noise, all of infinitesimal amplitude. Though they used the mean as the final decomposition of the Dirac pulse, they defined the true answer as

$$d[n] = \lim_{e \to 0^+} E\{d[n] + \varepsilon r_k[n]\}, \tag{2}$$

in which, $[n]$ represents nth data point, $d[n]$ is the Dirac function, $r_k[n]$ is a random number, ε is the infinitesimal parameter, and $E\{\ \}$ is the expected value. Flandrin's novel use of the added noise has made the EMD algorithm operable for a data set that could not be previously analyzed.

Another novel use of noise in data analysis is by Gledhill,[8] who used noise to test the robustness of the EMD algorithm. Although an ensemble of noise was used, he never used the cancellation principle to define the ensemble mean as the true answer. Based on his discovery (that noise could cause the EMD to produce slightly different outcomes), he assumed that the result from the clean data without noise was the true answer and thus designated it as the reference. He then defined the discrepancy, Δ, as

$$\Delta = \sum_{j=1}^{m} \left(\sum_{t} (cr_j(t) - cn_j(t))^2 \right)^{1/2}, \tag{3}$$

where cr_j and cn_j are the jth component of the IMF without and with noise added, and m is the total number of IMFs generated from the data. In his extensive study of the detailed distribution of the noise-caused "discrepancy," he concluded that the EMD algorithm is reasonably stable for small perturbations. This conclusion is in slight conflict with his observations that the perturbed answer with infinitesimal noise showed a bimodal distribution of the discrepancy.

Gledhill had also pushed the noise-added analysis in another direction: he had proposed to use an ensemble mean of noise-added analysis to form a "Composite Hilbert spectrum." As the spectrum is non-negative, the added noise could not cancel out. He then proposed to keep a noise-only spectrum and subtract it from the full noise-added spectrum at the end. This non-cancellation of noise in the spectrum, however, forced Gledhill[8] to limit the noise used to be of small magnitude, so that he could be sure that there would not be too much interaction between the noise-added and the original clean signal, and that the contribution of the noise to the final energy density in the spectrum would be negligible.

Although noise of infinitesimal amplitude used by Gledhill[8] has improved the confidence limit of the final spectrum, Gledhill explored neither fully the cancellation property of the noise nor the power of finite perturbation to explore all possible solutions. Furthermore, it is well known that whenever there is intermittence, the signal without noise can produce IMFs with mode mixing. There is no justification to assume that the result without added noise is the truth or the reference signal. These reservations notwithstanding, all these studies by Flandrin *et al.*[7] and Gledhill[8] had still greatly advanced the understanding of the effects of noise in the EMD method, though the crucial effects of noise had yet to be clearly articulated and fully explored.

In the following, the new noise-added EMD approach will be explained, in which the cancellation principle will be fully utilized, even with finite amplitude noise. Also emphasized is the finding that the true solution of the EMD method should be the

ensemble mean rather than the clean data. This full presentation of the new method will be the subject of the next section.

3. Ensemble Empirical Mode Decomposition

3.1. *The empirical mode decomposition*

This section starts with a brief review of the original EMD method. The detailed method can be found in the works of Huang *et al.*[1] and Huang *et al.*[2] Different to almost all previous methods of data analysis, the EMD method is adaptive, with the basis of the decomposition based on and derived from the data. In the EMD approach, the data $X(t)$ is decomposed in terms of IMFs, c_j, i.e.,

$$x(t) = \sum_{j=1}^{n} c_j + r_n, \tag{4}$$

where r_n is the residue of data $x(t)$, after n number of IMFs are extracted. IMFs are simple oscillatory functions with varying amplitude and frequency, and hence have the following properties:

1. Throughout the whole length of a single IMF, the number of extrema and the number of zero-crossings must either be equal or differ at most by one (although these numbers could differ significantly for the original data set).
2. At any data location, the mean value of the envelope defined by the local maxima and the envelope defined by the local minima is zero.

In practice, the EMD is implemented through a sifting process that uses only local extrema. From any data r_{j-1}, say, the procedure is as follows: (1) identify all the local extrema (the combination of both maxima and minima) and connect all these local maxima (minima) with a cubic spline as the upper (lower) envelope; (2) obtain the first component h by taking the difference between the data and the local mean of the two envelopes; and (3) Treat h as the data and repeat steps 1 and 2 as many times as is required until the envelopes are symmetric with respect to zero mean under certain criteria. The final h is designated as c_j. A complete sifting process stops when the residue, r_n, becomes a monotonic function from which no more IMFs can be extracted.

Based on this simple description of EMD, Flandrin *et al.*[5] and Wu and Huang[6] have shown that, if the data consisted of white noise which has scales populated uniformly through the whole timescale or time–frequency space, the EMD behaves as a dyadic filter bank: the Fourier spectra of various IMFs collapse to a single shape along the axis of logarithm of period or frequency. Then the total number of IMFs of a data set is close to $\log_2 N$ with N the number of total data points. When the data is not pure noise, some scales could be missing; therefore, the total number of the IMFs might be fewer than $\log_2 N$. Additionally, the intermittency of signals in certain scale would also cause mode mixing.

3.2. *Mode mixing problem*

"Mode mixing" is defined as any IMF consisting of oscillations of dramatically disparate scales, often caused by intermittency of the driving mechanisms. When mode mixing occurs, an IMF can cease to have physical meaning by itself, suggesting falsely that there may be different physical processes represented in a mode. Even though the final time–frequency projection could rectify the mixed mode to some degree, the alias at each transition from one scale to another would irrecoverably damage the clean separation of scales. Such a drawback was first illustrated by Huang *et al.*[2] in which the modeled data was a mixture of intermittent high-frequency oscillations riding on a continuous low-frequency sinusoidal signal. An almost identical example used by Huang *et al.*[2] is presented here in detail as an illustration.

The data and its sifting process are illustrated in Fig. 1. The data has its fundamental part as a low-frequency sinusoidal wave with unit amplitude. At the three

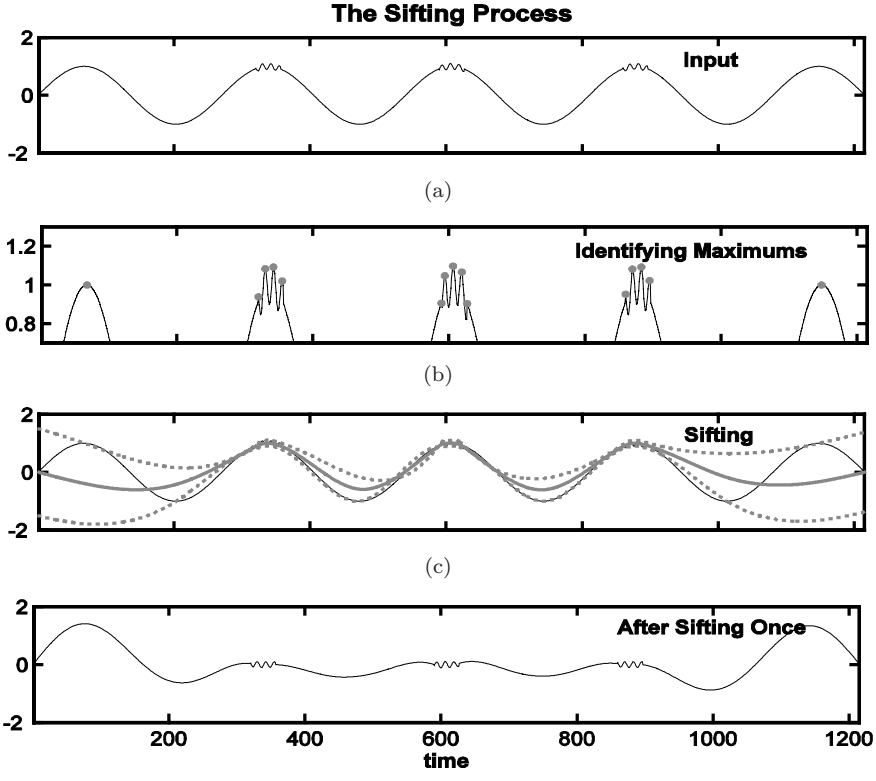

Fig. 1. The very first step of the sifting process. Panel (a) is the input; panel (b) identifies local maxima (gray dots); panel (c) plots the upper envelope (upper gray dashed line) and low envelope (lower gray dashed line) and their mean (bold gray line); and panel (d) is the difference between the input and the mean of the envelopes.

middle crests of the low-frequency wave, high-frequency intermittent oscillations with an amplitude of 0.1 are riding on the fundamental, as panel (a) of Fig. 1 shows. The sifting process starts with identifying the maxima (minima) in the data. In this case, 15 local maxima are identified, with the first and the last coming from the fundamental, and the other 13 caused mainly by intermittent oscillations (panel (b)). As a result, the upper envelope resembles neither the upper envelope of the fundamental (which is a flat line at one) nor the upper one of the intermittent oscillations (which is supposed to be the fundamental outside intermittent areas). Rather, the envelope is a mixture of the envelopes of the fundamental and of the intermittent signals that lead to a severely distorted envelope mean (the thick gray line in panel (c)). Consequently, the initial guess of the first IMF (panel (d)) is the mixture of both the low-frequency fundamental and the high-frequency intermittent waves, as shown in Fig. 2.

An annoying implication of such scale mixing is related to unstableness and lack of the uniqueness of decomposition using the EMD. With stoppage criterion given and end-point approach prescribed in the EMD, the application of the EMD to any real data results in a unique set of IMFs, just as when the data is processed by other data decomposition methods. This uniqueness is here referred to as "the mathematical uniqueness," and satisfaction to the mathematical uniqueness is the minimal requirement for any decomposition method. The issue that is emphasized

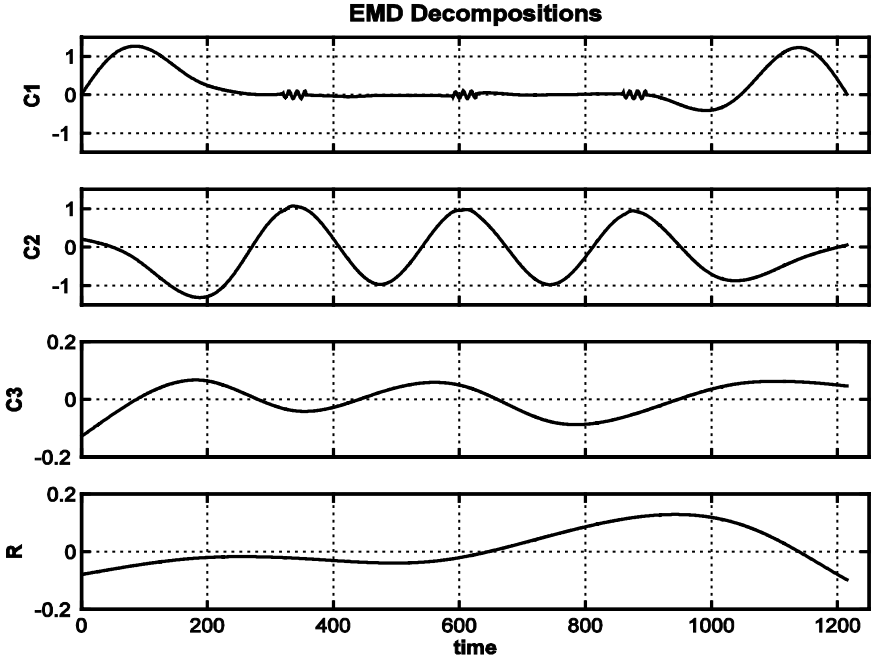

Fig. 2. The intrinsic mode functions of the input displayed in Fig. 1(a).

here is what we refer to as "the physical uniqueness." Since real data almost always contains a certain amount of random noise or intermittences that are not known to us, an important issue, therefore, is whether the decomposition is sensitive to noise. If the decomposition is insensitive to added noise of small but finite amplitude and bears little quantitative and no qualitative change, the decomposition is generally considered stable and satisfies the physical uniqueness; and otherwise, the decomposition is unstable and does not satisfy the physical uniqueness. The result from decomposition that does not satisfy the physical uniqueness may not be reliable and may not be suitable for physical interpretation. For many traditional data decomposition methods with prescribed base functions, the uniqueness of the second kind is automatically satisfied. Unfortunately, the EMD in general does not satisfy this requirement due to the fact that decomposition is solely based on the distribution of extrema.

To alleviate this drawback, Huang *et al.*[2] proposed an intermittence test that subjectively extracts the oscillations with periods significantly smaller than a preselected value during the sifting process. The method works quite well for this example. However, for complicated data with scales variable and continuously distributed, no single criterion of intermittence test can be selected. Furthermore, the most troublesome aspect of this subjectively pre-selected criterion is that it lacks physical justifications and renders the EMD nonadaptive. Additionally, mode mixing is also the main reason that renders the EMD algorithm unstable: any small perturbation may result in a new set of IMFs as reported by Gledhill.[8] Obviously, the intermittence prevents EMD from extracting any signal with similar scales. To solve these problems, the EEMD is proposed, which will be described in the following sections.

3.3. *Ensemble empirical mode decomposition*

As given in Eq. (1), all data are amalgamations of signal and noise. To improve the accuracy of measurements, the ensemble mean is a powerful approach, where data are collected by separate observations, each of which contains different noise. To generalize this ensemble idea, noise is introduced to the single data set, $x(t)$, as if separate observations were indeed being made as an analog to a physical experiment that could be repeated many times. The added white noise is treated as the possible random noise that would be encountered in the measurement process. Under such conditions, the ith "artificial" observation will be

$$x_i(t) = x(t) + w_i(t). \tag{5}$$

In the case of only one observation, each multiple-observation ensembles is mimicked by adding not arbitrary but different realizations of white noise, $w_i(t)$, to that single observation as given in Eq. (5). Although adding noise may result in smaller signal-to-noise ratio, the added white noise will provide a relatively uniform reference scale distribution to facilitate EMD; therefore, the low signal–noise ratio

does not affect the decomposition method but actually enhances it to avoid the mode mixing. Based on this argument, an additional step is taken by arguing that adding white noise may help to extract the true signals in the data, a method that is termed EEMD, a truly NADA method.

Before looking at the details of the new EEMD, a review of a few properties of the original EMD is presented:

1. the EMD is an adaptive data analysis method that is based on local characteristics of the data, and hence, it catches nonlinear, nonstationary oscillations more effectively;
2. the EMD is a dyadic filter bank for any white (or fractional Gaussian) noise-only series;
3. when the data is intermittent, the dyadic property is often compromised in the original EMD as the example in Fig. 2 shows;
4. adding noise to the data could provide a uniformly distributed reference scale, which enables EMD to repair the compromised dyadic property; and
5. the corresponding IMFs of different series of noise have no correlation with each other. Therefore, the means of the corresponding IMFs of different white noise series are likely to cancel each other.

With these properties of the EMD in mind, the proposed EEMD is developed as follows:

1. add a white noise series to the targeted data;
2. decompose the data with added white noise into IMFs;
3. repeat step 1 and step 2 again and again, but with different white noise series each time; and
4. obtain the (ensemble) means of corresponding IMFs of the decompositions as the final result.

The effects of the decomposition using the EEMD are that the added white noise series cancel each other in the final mean of the corresponding IMFs; the mean IMFs stay within the natural dyadic filter windows and thus significantly reduce the chance of mode mixing and preserve the dyadic property.

To illustrate the procedure, the data in Fig. 1 is used as an example. If the EEMD is implemented with the added noise having an amplitude of 0.1 standard deviation of the original data for just one trial, the result is given in Fig. 3. Here, the low-frequency component is already extracted almost perfectly. The high-frequency components, however, are buried in noise. Note that high-frequency intermittent signal emerges when the number of ensemble members increases, as Fig. 4 displays. Clearly, the fundamental signal C5 is represented nearly perfect, as well as the intermittent signals, if C2 and C3 are added together. The fact that the intermittent signal actually resides in two EEMD components is due to the average spectra of neighboring IMFs of white noise overlapping, as revealed by Wu

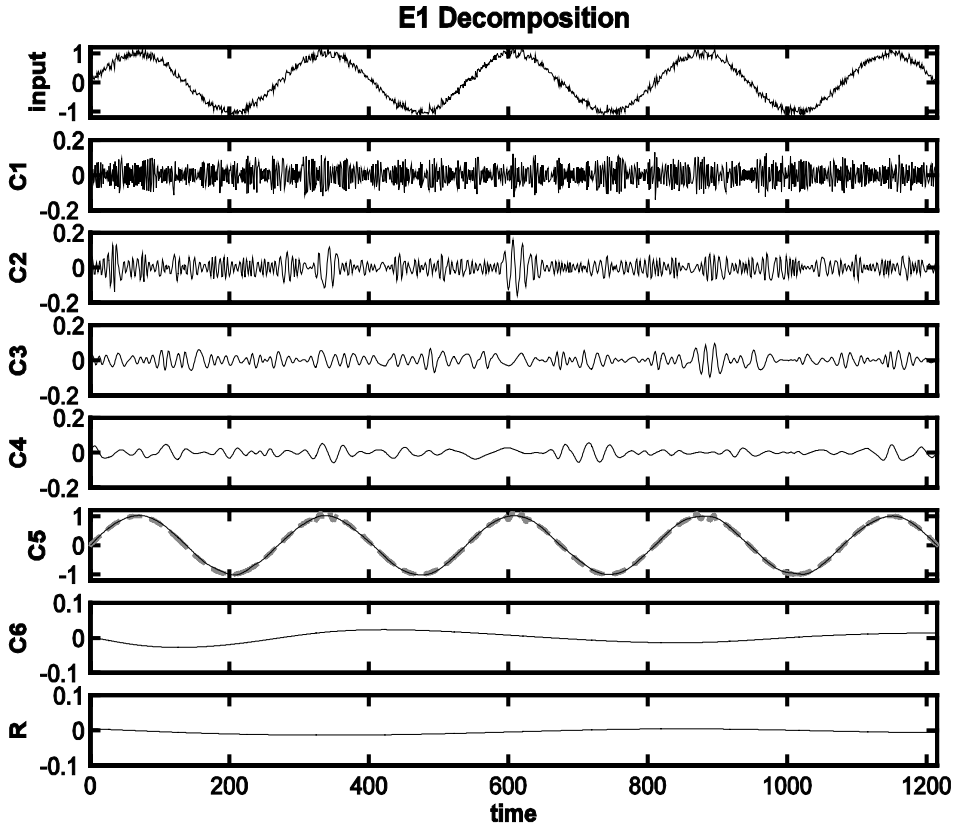

Fig. 3. The modified input (the top panel), its intrinsic mode functions (C1–6), and the trend of (R). In panel C5, the original input is plotted as the bold dashed gray line for comparison.

and Huang.[6] Thus sometimes, the combination of two adjutant components to form one IMF is necessary. The need for this type of adjustment is easily determined through an orthogonality check. Whenever two IMF components become grossly unorthogonal, one should consider combining the two to form a single IMF component.

This provides the first example to demonstrate that the NADA, using the EEMD significantly, improves the capability of extracting signals in the data, and represents a major improvement of the EMD method.

4. Real World Examples

The previous example introduced the concept of NADA using the EEMD method. The question now is whether the EEMD indeed helps in reaching the ultimate goal of data analysis: to isolate and extract the physically meaningful signals in data, and thereby to understand the properties of data and its underlying physics. The easiest way to demonstrate the power of the EEMD and its usefulness is to apply

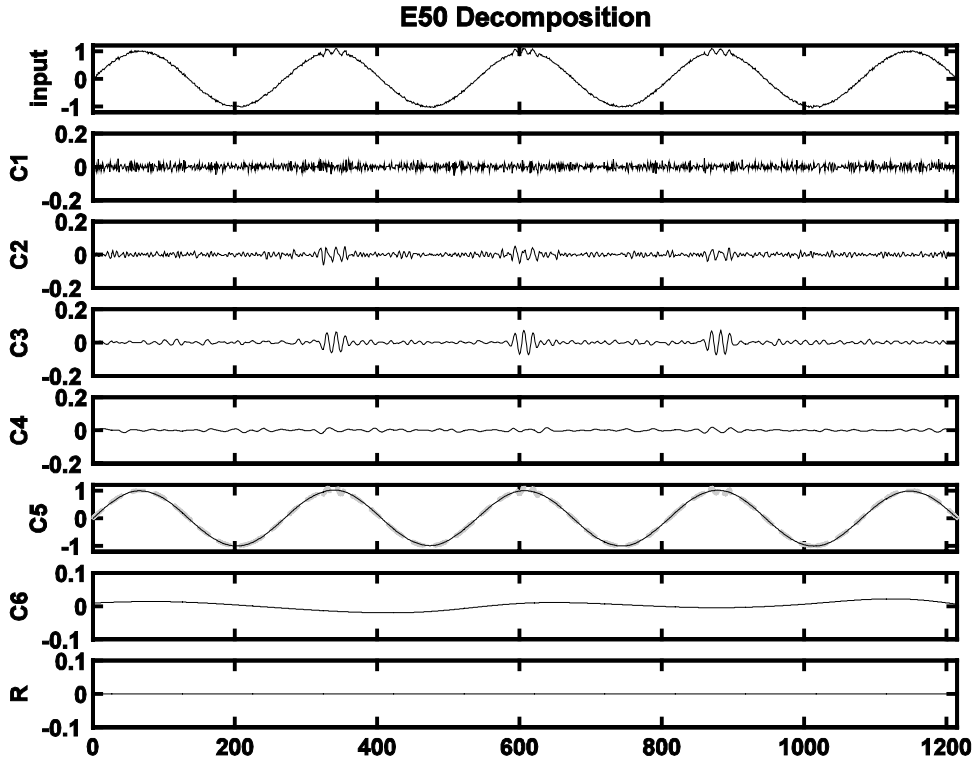

Fig. 4. The IMF-like components of the decomposition of the original input in the top panel of Fig. 1 using the EEMD. In the EEMD, an ensemble member of 50 is used, and the added white noise in each ensemble member has a standard deviation of 0.1. In the top panel, the mean of the noise-modified input is plotted. In panel C5, the original input (gray line) is also displayed for comparison.

to data of natural phenomena. In this section, EEMD is applied to two real cases: the first one is climate data that define the interaction between atmosphere and ocean; and the second one is a section of a high resolution digitalized sound record. Both cases are complicated and have rich properties in the data. These data are considered general enough to be the representatives of real cases.

4.1. *Example 1: Analysis of climate data*

The first set of data to be examined here is representative of an interacting air–sea system in the tropics known as the El Niño-Southern Oscillation (ENSO) phenomenon. The Southern Oscillation (SO) is a global-scale seesaw in atmospheric pressure between the western and the southeastern tropical Pacific, and the El Niño refers to variations in temperature and circulation in the tropical Pacific Ocean. The two systems are closely coupled,[24,25] and together they produce important climate fluctuations that have a significant impact on weather and climate over the globe

as well as social and economic consequences (see, e.g., Ref. 26). The underlying physics of ENSO have been explained in numerous papers (see, e.g., Refs. 27–29).

The Southern Oscillation is often represented by the Southern Oscillation Index (SOI), a normalized monthly sea level pressure index based on the pressure records collected in Darwin, Australia, and Tahiti Island in the eastern tropical Pacific.[30] It should be noted here that the Tahiti record used for the calculation of SOI is less reliable and contains missing data prior to 1935. The Cold Tongue Index (CTI), defined as the average large year-to-year SST anomaly fluctuations over 6°N–6°S, 180–90°W, is a good representation of El Niño.[31] A large negative peak of SOI, which often occurs with a two- to seven-year period, corresponds to a strong El Niño (warm) event. With its rich statistical properties and scientific importance, the SOI is one of the most prominent time series in the geophysical research community and has been well studied. Many time-series analysis tools have been used on this time series to display their capability of revealing useful scientific information.[6,32,33] The specific question to be examined here is over what timescales are the El Niño and the Southern Oscillation coupled?

The SOI used in this study is described in the works of Ropelewski and Jones[34] and Allan *et al.*[35] The CTI is based on the SST from January 1870 to December 2002 provided by the Hadley Center for Climate Prediction and Research,[36] which is refined from direct observations. The sparse and low-quality observations in the early stages of the period make the two indices in the early stages less consistent and their interrelationship less reliable, as reflected by the fact that the overall correlations between the two time series is −0.57 for the whole data length, but only −0.45 for the first half, and −0.68 for the second half. The two indices of the second half are plotted in Fig. 5.

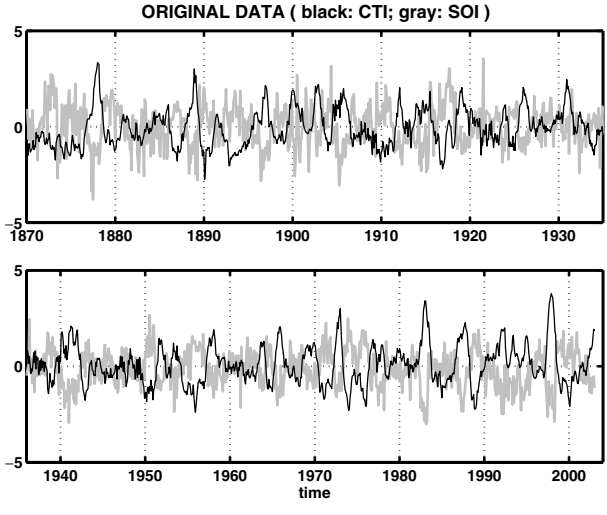

Fig. 5. The Southern Oscillation Index (gray line) and the Cold Tongue Index (black line).

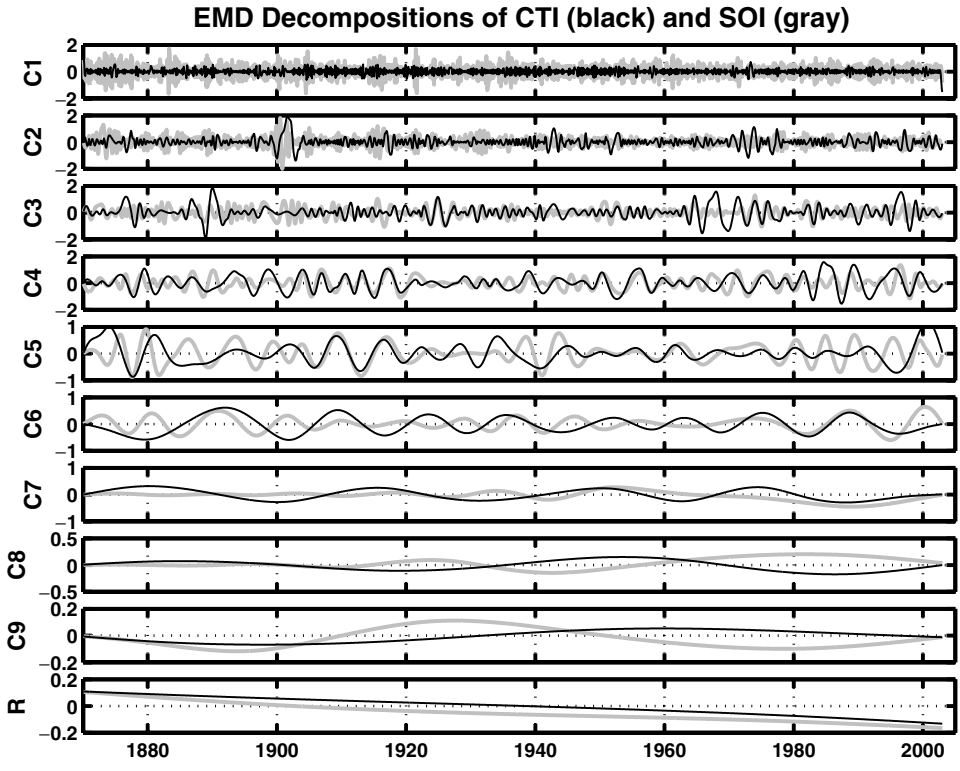

Fig. 6. The intrinsic mode functions and the trends of the Southern Oscillation Index (gray lines) and the Cold Tongue Index (black lines). For the convenience of identifying their synchronization, the CTI and its components are flipped in sign.

The decompositions of these two indices using the original EMD are plotted in Fig. 6. Although SOI and CTI have a quite large correlation (−0.57), their corresponding IMFs, however, show little synchronization. For the whole data length, the largest negative correlation amongst the IMFs is only −0.43 (see Fig. 7), a much smaller value than that of the correlation between the whole data of SOI and CTI. Since the underlying physical processes that dictate the large-scale interaction between atmosphere and ocean differ on various timescales, a good decomposition method is expected to identify such variations. However, the low correlations between corresponding IMFs seem to indicate that the decompositions using the original EMD on SOI and CTI help little to identify and understand which timescales for the coupling between atmosphere and ocean in climate system in the tropics are more prominent.

This lack of correlation clearly represents a typical problem of mode mixing in the original EMD. From a visual inspection, it is easily seen that in almost any high- or middle-scale IMF of SOI or CTI, pieces of oscillations having approximate periods of those appear also in its neighboring IMFs. The mixing is also contagious: if it

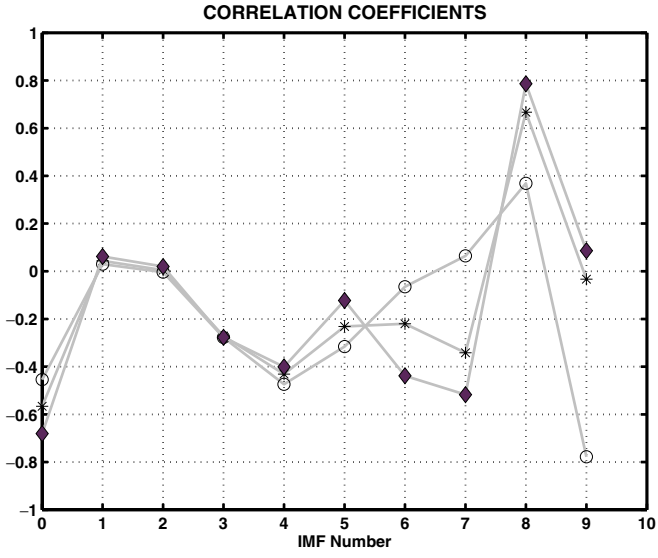

Fig. 7. The correlation coefficients of the SOI and CTI and their corresponding IMFs. IMF 0 here means the original signal. The asterisks are for the whole data length; the circles are for the first half; and the diamonds for the second half. The horizontal axis plots the order of IMFs.

happens in one IMF, it will happen in the following IMFs at the same temporal neighborhood. Consequently, mode mixing reduces the capability of the EMD in identifying the true timescales of consistent coupled oscillations in the individual IMF component in the ENSO system. This is clearly shown in Fig. 7, in which none of the IMF pairs with a rank from 1 to 7 have a higher correlation than the full data set.

To solve this problem and to identify the timescale at which the interaction truly occurs, both time series were reanalyzed using the EEMD. The results are displayed in Fig. 8. It is clear that the synchronizations between corresponding IMF pairs are much improved, especially for the IMF components 4–7 in the latter half of the record. As mentioned earlier, both SOI and CTI are not as reliable in the first half of the record as those in the second half due to the sparse or missing observations. Therefore, the lower degree of synchronization of the corresponding IMF components of SOI and of CTI in the earlier half is not likely caused by EEMD, but by the less consistent data of SOI and CTI in that period. To quantify this claim, the detailed correlation values of the corresponding IMF pairs will be discussed next.

The detailed correlation between the corresponding IMF components of SOI and CTI are displayed in Fig. 9. Clearly, the decompositions using the EEMD improve the correlation values significantly. The EEMD results help greatly in the isolation of signals of various scales that reflect the coupling between atmosphere and ocean in the ENSO system. Consistently high correlations between IMFs from

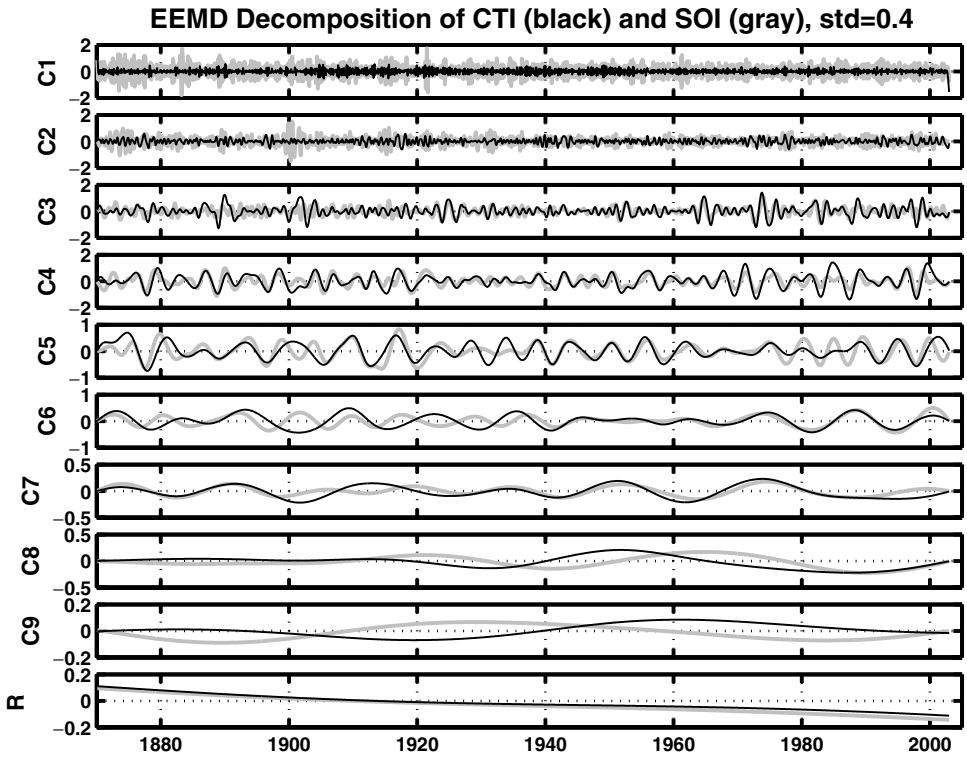

Fig. 8. The IMF-like components of the decompositions of the SOI (gray lines) and the CTI (black lines) using the EEMD. In the EEMD, an ensemble size of 100 is used, and the added white noise in each ensemble member has a standard deviation of 0.4. For the convenience of identifying their synchronization, the CTI and its components are flipped in sign.

SOI and CTI on various timescales have been obtained, especially those of interannual (components 4 and 5 with mean periods of 2.83 and 5.23 years, respectively) and short interdecadal (components 6 and 7 with mean periods of 10.50 and 20.0 years, respectively) timescales. The increase of the correlation coefficients from just under 0.68 for the latter half of the whole data to significantly over 0.8 for these IMF pairs is remarkable. There has not yet been any other filtering method used to study these two time series that has led to such high correlations between the band-filtered results from published literature on all these timescales. (For the long interdecadal timescales, especially for C8 and C9, since the number of degrees of freedom of the IMF components is very small due to the lack of oscillation variations, the correlation coefficients corresponding to them can be very misleading; therefore, they should be ignored.) These results clearly indicate the most important coupling between the atmosphere and the ocean that occurs on a broad range of timescales, covering interannual and interdecadal scales from 2 to 20 years.

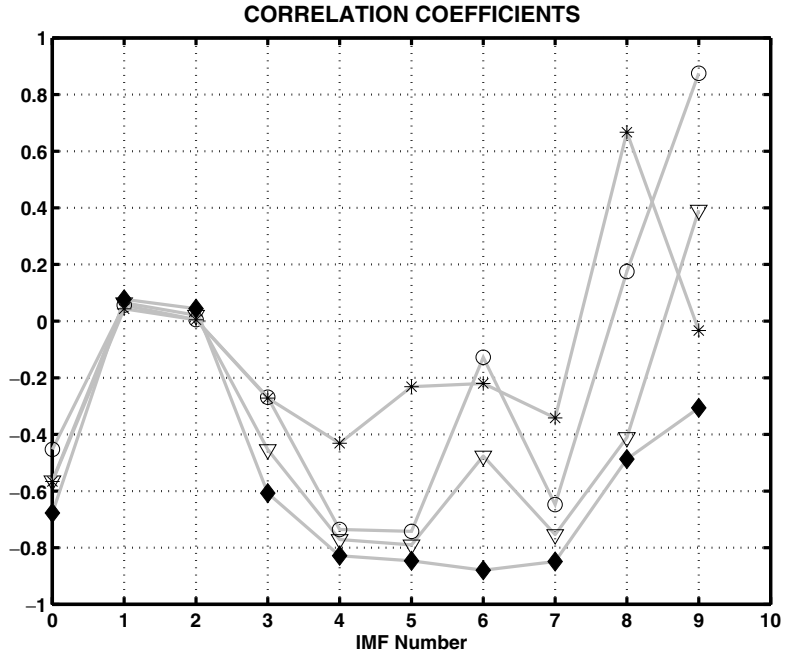

Fig. 9. The correlation coefficients of the SOI and CTI and their corresponding IMF-like components. IMF 0 here means the original signal. The triangles are for the whole data length; the circles for the first half; and the diamonds for the second half. The asterisks are the same as the corresponding asterisks in Fig. 7, i.e., the correlation coefficients of SOI and CTI and their corresponding IMFs obtained with the original EMD for the whole data length. The horizontal axis plots the order of IMFs.

The high correlations on interannual and short interdecadal timescales between IMFs of SOI and CTI, especially in the latter half of the record, are consistent with the physical explanations provided by recent studies. These IMFs are statistically significant at 95% confidence level based on a testing method proposed by Wu and Huang[6,9] against the white noise null hypothesis. The two interannual modes (C4 and C5) are also statistically significant at 95% confidence level against the traditional red noise null hypothesis. Indeed, Jin *et al.* (personal communications, their manuscript being under preparation) have solved a nonlinear coupled atmosphere–ocean system and showed analytically that the interannual variability of ENSO has two separate modes with periods in agreement with the results obtained here. Concerning the coupled short interdecadal modes, they are also in good agreement with a recent modeling study by Yeh and Kirtman,[37] which demonstrated that such modes can be a result of a coupled system in response to stochastic forcing. Therefore, the EEMD method does provide a more powerful tool to isolate signals of specific timescales in observational data produced by different underlying physics.

4.2. *Example 2: Analysis of voice data*

In the previous example, the demonstration of power and confirmation of the usefulness of the EEMD was made through analyzing two different but physically closely interacted subsystems (corresponding to two different data sets) of a climate system. Such a pair of highly related data sets is rare in more general cases of signal processing. Therefore, to further illustrate the EEMD as an effective data analysis method in time–frequency domain for general purpose, we analyze a piece of speech data using the EEMD. The original data, given in Fig. 10, shows the digitalized sound of the word, "Hello," at 22 050 Hz digitization.[38]

The EMD components obtained from the original EMD without added noise is given in Fig. 11. Here, we can see mode mixing from the second component and down, where highly disparate amplitudes and scales are evident. The mode mixing influences the scale parity in all the IMF components, though some are not as obvious.

The same data was then processed with the EEMD with a noise selected at an amplitude of 0.1 times that of the data RMS, and 1000 trials. The result is a drastic improvement, as shown in Fig. 12. Here, all the IMF-like components are continuous and without any obvious fragmentation. The third component is almost the full signal, which can produce a sound that is clear and with almost the original audio quality. All other components also have relatively uniform scales, but the sounds produced by them are not intelligible: they mostly consist of either high-frequency hissing or low-frequency moaning. The results once again clearly demonstrate that the EEMD has the capability of catching the essence of data that manifests the underlying physics.

The improvements on the quality of the IMFs also have drastic effects on the time–frequency distribution of the data in Hilbert spectra, as shown in Figs. 13

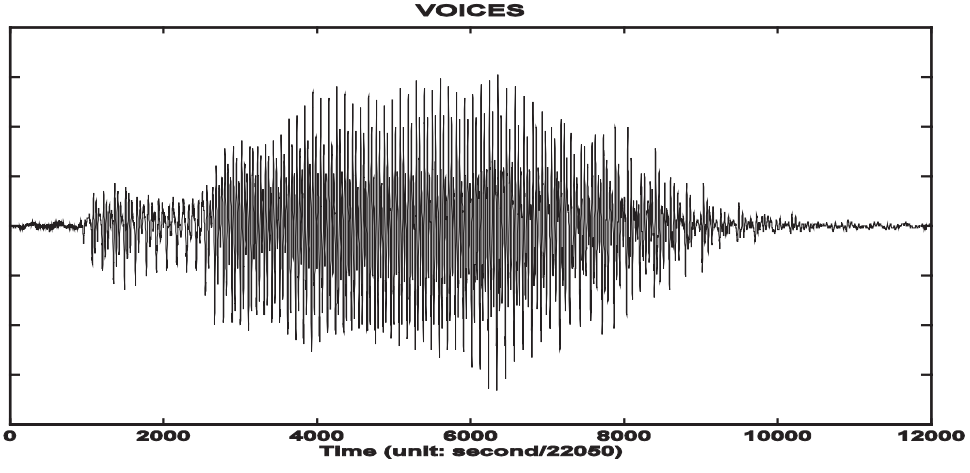

Fig. 10. Digitalized sound of the word, "Hello," at 22 050 Hz.

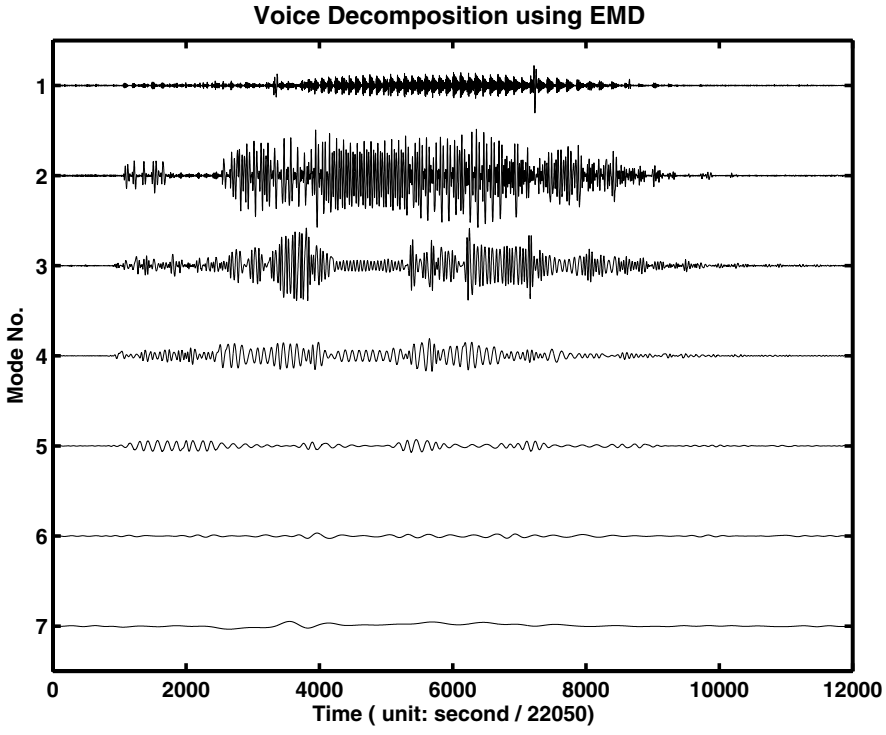

Fig. 11. The IMFs (C1–C7, from the top to the bottom, respectively) of digitalized sound "Hello" from the EMD without added noise. C7 includes all the low-frequency part not represented by C1–C6. The mode mixing has caused the second and third components to intersperse with the sections of data having highly disparate amplitudes and scales.

and 14 for EMD and EEMD results of the voice data, respectively. In the original EMD, the mode mixings have caused the time–frequency distribution to be fragmentary. The alias at the transition points from one scale to another is clearly visible. Although the Hilbert spectra of this quality could be used for some general purposes such as identifying the basic frequencies and their ranges of variation, quantitative measures would be extremely difficult. The Hilbert spectrum from the EEMD shows a great improvement. The mode mixing has almost completely disappeared. There are almost no transition gaps, and all basic frequency traces are continuous in the time–frequency space. It is noted here that to obtain the Hilbert spectrum of EEMD components, the post-EEMD processing is applied, which is described in Sec. 5.3.

For comparison, wavelet packet decomposition (WPD) result of "Hello" is presented in Fig. 15. In this decomposition, we have tried a few wavelets. We found that "Meyer wavelet" provides the best results because of its oscillatory shape fitting well to the local oscillations of voice. Since each component resulted from WPD has a fixed scale, there is no scale-mixing problem. However, due to the rigidly fixed

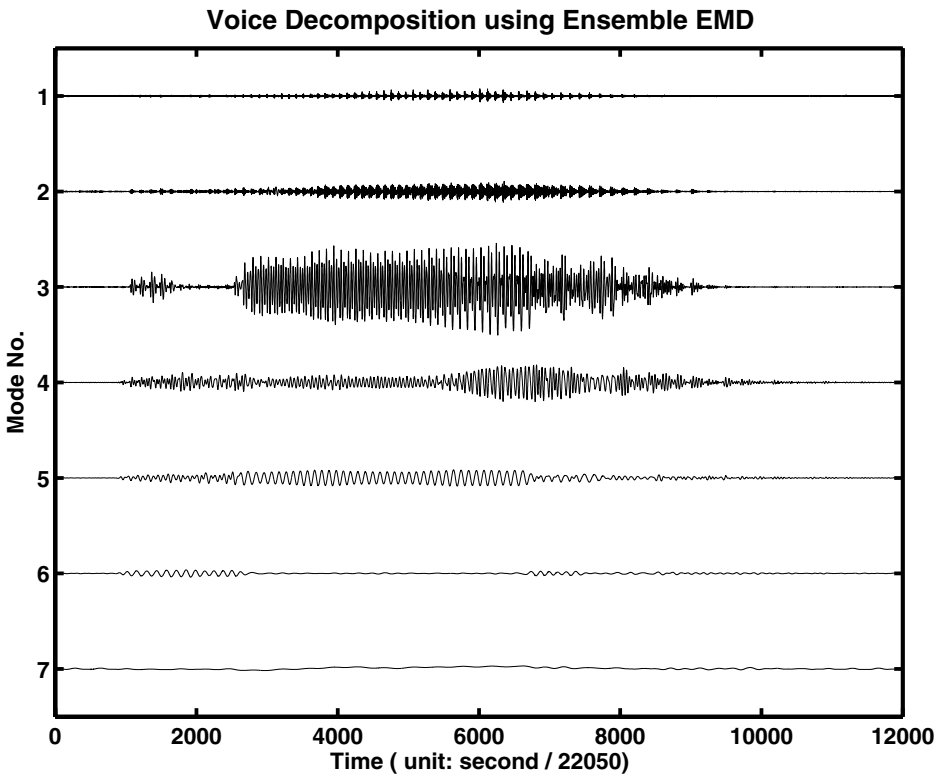

Fig. 12. Same as in Fig. 11, but the components are obtained using EEMD.

wavelet shape, part of voice that has local oscillation not matching the wavelet shape cannot be represented well by the WPD decomposition.

To obtain an impression of how efficient are EMD, EEMD, and WPD to catch the physically meaningful information hidden in voice data, the dominant components from various decompositions are plotted in Fig. 16. In EMD decompositions, two different stoppage criteria are used: one is the repeat of three times of S-number[39] and the other is to fix the sifting number to 10. The effect of different stoppage criteria on EMD decomposition will be discussed in App. A. From a visual inspection, one may conclude that EEMD provides the most efficient decomposition and WPD is the second. Indeed, the dominant EEMD component represents a superb voice compared to those dominant components from EMD and WPD. However, if the voices of the EMD and WPD components are compared, one may conclude that EMD decomposition with local stoppage criterion (a sifting number fixed to 10) is more efficient than WPD, implying that the adaptive representation may be a better choice to represent the essence of voice and the popular harmonic representation of voice (such as in WPD) has

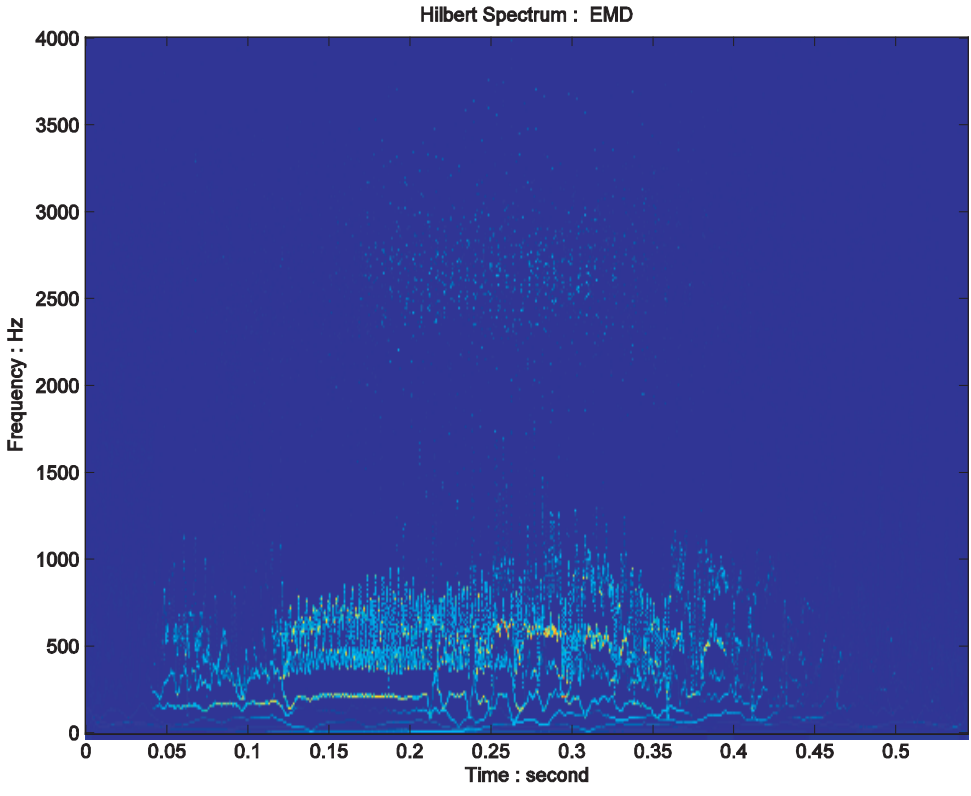

Fig. 13. The Hilbert spectrum from the original EMD without added noise. The mode mixing has caused numerous transition gaps, and rendered the time–frequency traces fragmented.

fundamental drawbacks. However, when a global stoppage criterion (such as prescribing S-number to 3) is used, the mode mixing is severe, and the dominant component catches little of the essence of voice. (Readers who want to listen to the voices of these dominant components, could contact the authors of this paper.)

5. Some Issues of EEMD

The previous sections have introduced the EEMD method and its capability of extracting physically meaning components from data. However, in EEMD, the number of ensemble and the noise amplitude are the two parameters that need to be prescribed. In addition to that, since the ensemble mean of the corresponding IMFs from individual EMD decomposition is not necessary an IMF, the Hilbert spectrum analysis of EEMD components may not be feasible. In this section, we will discuss these issues.

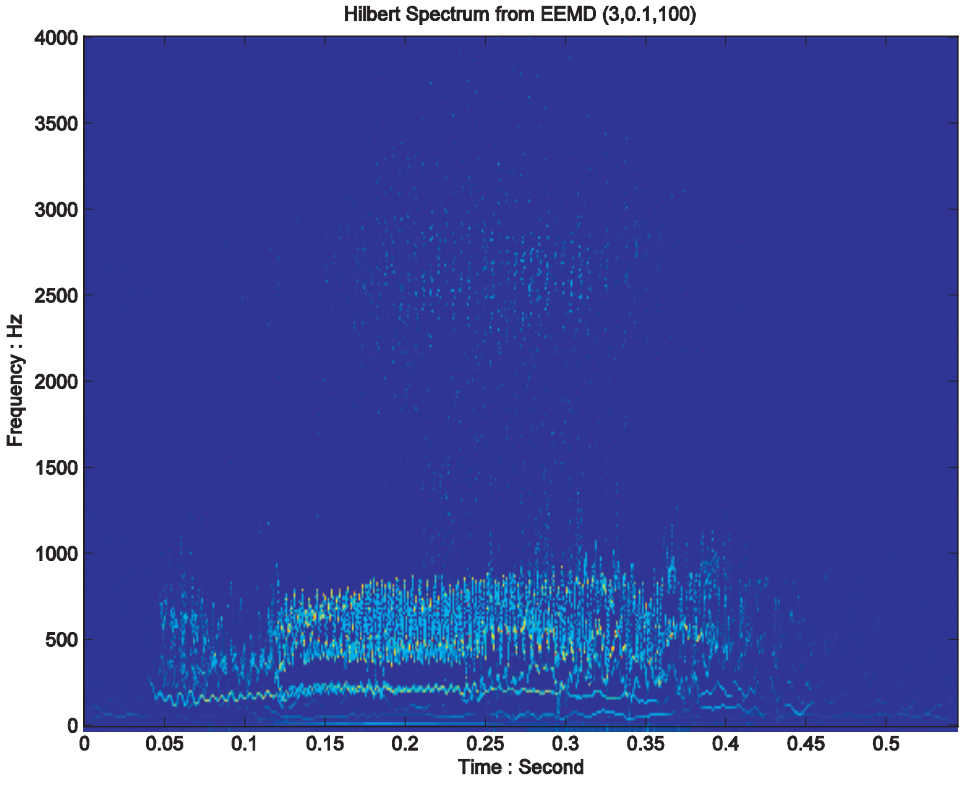

Fig. 14. The Hilbert spectrum from the EEMD with added noise.

5.1. *The number of ensemble for EEMD*

The effect of the added white noise should decrease following the well-established statistical rule:

$$\varepsilon_n = \frac{\varepsilon}{\sqrt{N}}, \tag{6a}$$

or

$$\ln \varepsilon_n + \frac{\varepsilon}{2} \ln N = 0, \tag{6b}$$

where N is the number of ensemble members, ε is the amplitude of the added noise, and ε_n is the final standard deviation of error, which is defined as the difference between the input signal and the corresponding IMF(s). Such a relation is clear in Fig. 17, in which the standard deviation of error is plotted as a function of the number of ensemble members. In general, the results agree well with the theoretical prediction. The relatively large deviation for the fundamental signal from the theoretical line fitting is understandable: the spread of error for low-frequency signals is large, as pointed by Wu and Huang.[6]

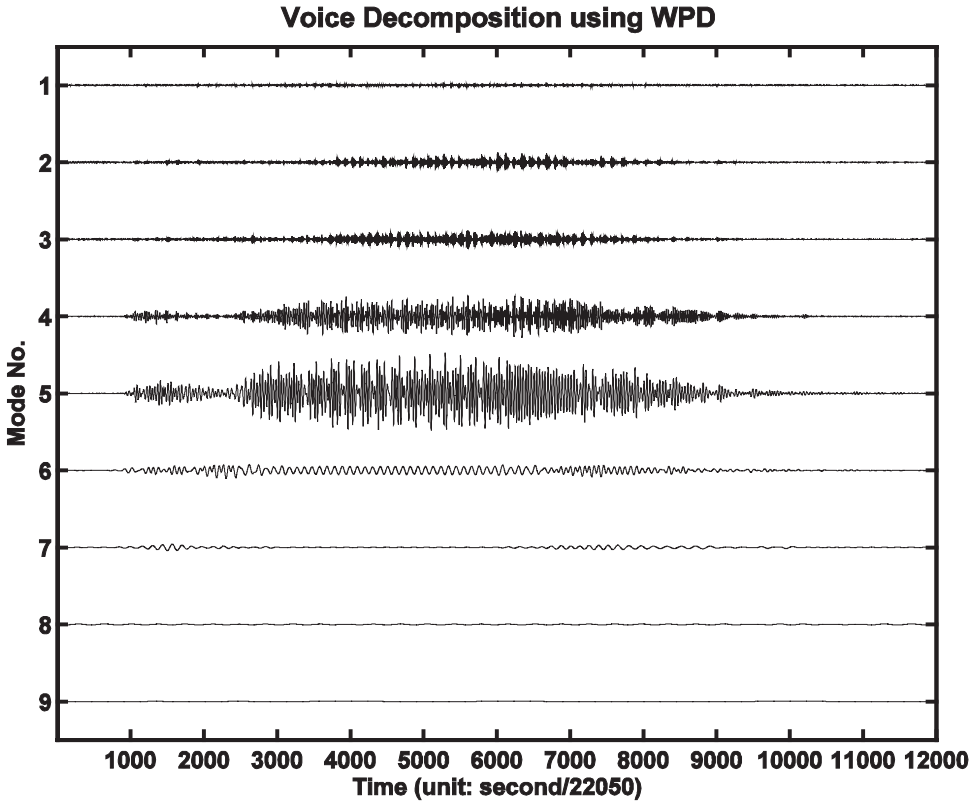

Fig. 15. The wavelet components (C1–C9, from the top to the bottom, respectively) of digitalized sound "Hello" from the EMD without added noise. C9 includes all the low frequency part not represented by C1–C8. In the wavelet packet decomposition, "Meyer wavelet" is used.

In fact, if the added noise amplitude is too small, then it may not introduce the change of extrema that the EMD relies on. This is true when the data have large gradient. Therefore, to make the EEMD effective, the amplitude of the added noise should not be too small. However, by increasing the ensemble members, the effect of the added white noise can be reduced to a negligibly small level. In general, an ensemble number of a few hundred will lead to a very good result, and the remaining noise would cause only less than a fraction of 1% of error if the added noise has an amplitude that is a fraction of the standard deviation of the original data.

5.2. *The amplitude of added noise*

Within a certain window of noise amplitude, the sensitivity of the decomposition of data using the EEMD to the amplitude of noise is often small. In Figs. 18 and 19, noise with a standard deviation of 0.1, 0.2, and 0.4 is added. The ensemble size for each case is 100. Clearly, the synchronization between cases of different levels of

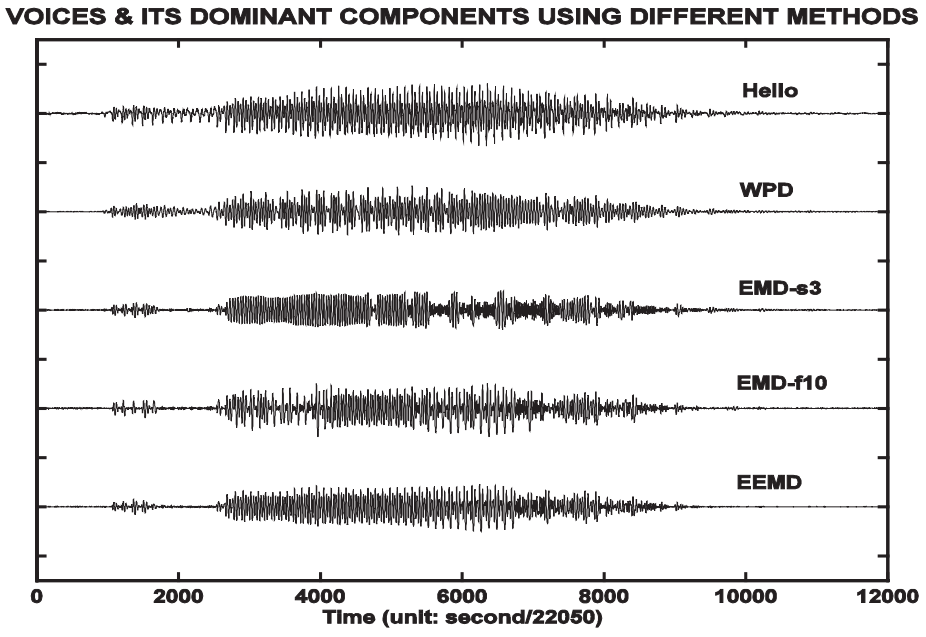

Fig. 16. The original digitalized voice data (marked with "Hello"), the dominant components of voice "Hello" from WPD (marked with "WPD"), from two EMD decompositions with different stoppage criteria (a criterion of repeating 3 times of S-number marked with "EMD-s3," see App. A for more details, and a criterion of fixing sifting number to 10 marked with "EMD-f10"), and from EEMD (marked with "EEMD").

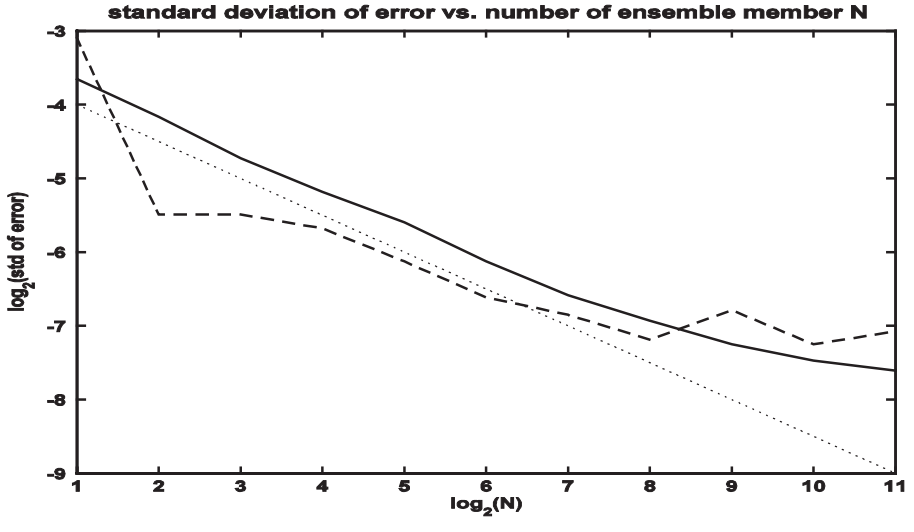

Fig. 17. The standard deviation of error as a function of the number of ensemble members. The solid line is for the high-frequency intermittent signals, and the dashed line is for the low-frequency fundamental signals. The dotted line is the theoretical line predicted by Eq. (6) with arbitrary vertical location, used as a reference.

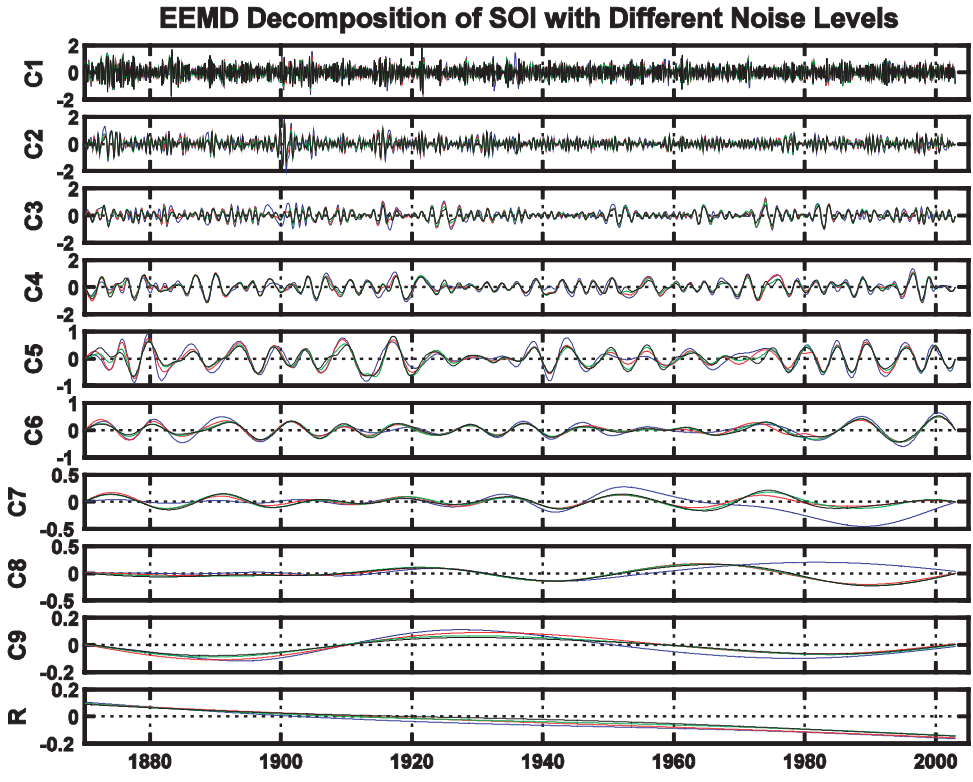

Fig. 18. EEMD decompositions of SOI with added noise. Blue line corresponds to the standard decomposition using EMD without any added noise. Red, green, and black lines correspond to EEMD decompositions with added noise of standard deviation of 0.1, 0.2, and 0.4, respectively. The ensemble number for each case is 100.

added noise is remarkably good, except the case of no noise added, in which mode mixing produced an unstable decomposition. In the latter case, any perturbation may push the result to a different state as studied by Gledhill.[8] Additionally, the improvement of the decomposition for CTI seems to be greater than that for SOI. The reason is simple: SOI is much noisier than CTI, since the former is based on noisy observations of sea level data from only two locations (Darwin and Tahiti pressures) while CTI is based on the averaged observed sea-surface temperature at hundreds of locations along the equator. This indeed indicates that EMD is a noise-friendly method: the noise contained in the data makes the EMD decomposition truly dyadic.

More decomposition of SOI and CTI with various noise levels and ensemble members has been carried out. The results (not shown here) indicate that increasing noise amplitudes and ensemble numbers alter the decomposition little as long as the added noise has moderate amplitude and the ensemble has a large enough number of trials. It should be noticed that the number of ensemble numbers should increase

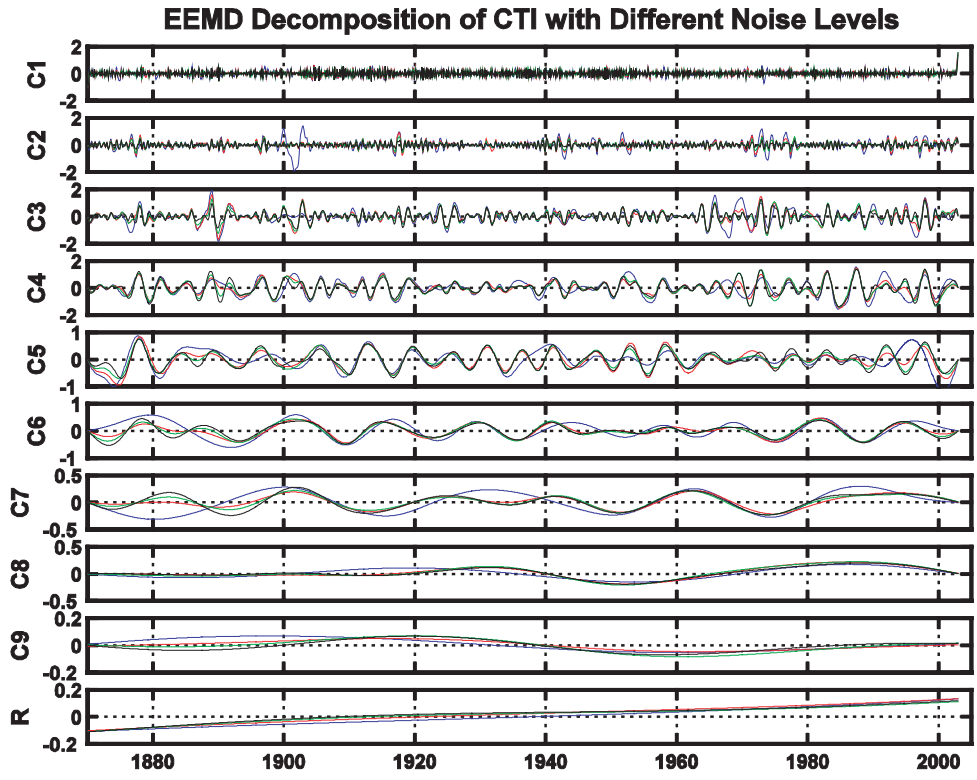

Fig. 19. EEMD decompositions of CTI with added noise. Blue line corresponds to the standard decomposition using EMD without any added noise. Red, green, and black lines correspond to EEMD decompositions with added noise of standard deviation of 0.1, 0.2, and 0.4, respectively. The ensemble number for each case is 100.

when the amplitude of noise increases so as to reduce the contribution of added noise in the decomposed results. The conclusions drawn for the decompositions of SOI and CTI here are also true for other data tried with the EEMD method. Therefore, the EEMD provides a sort of "uniqueness" and robustness result that the original EMD usually could not, and it also increases the confidence of the decomposition. In most cases, we suggest to add noise of an amplitude that is about 0.2 standard deviation of that of the data. However, when the data is dominated by high-frequency signals, the noise amplitude may be smaller, and when the data is dominated by low-frequency signals, the noise amplitude may be increased.

5.3. *Post processing of EEMD components*

As we mentioned earlier, the EEMD components of data are not necessarily IMFs, for EEMD involves numerous summations of IMFs. For such components, the corresponding Hilbert spectra can have significant alias. To overcome this drawback, we

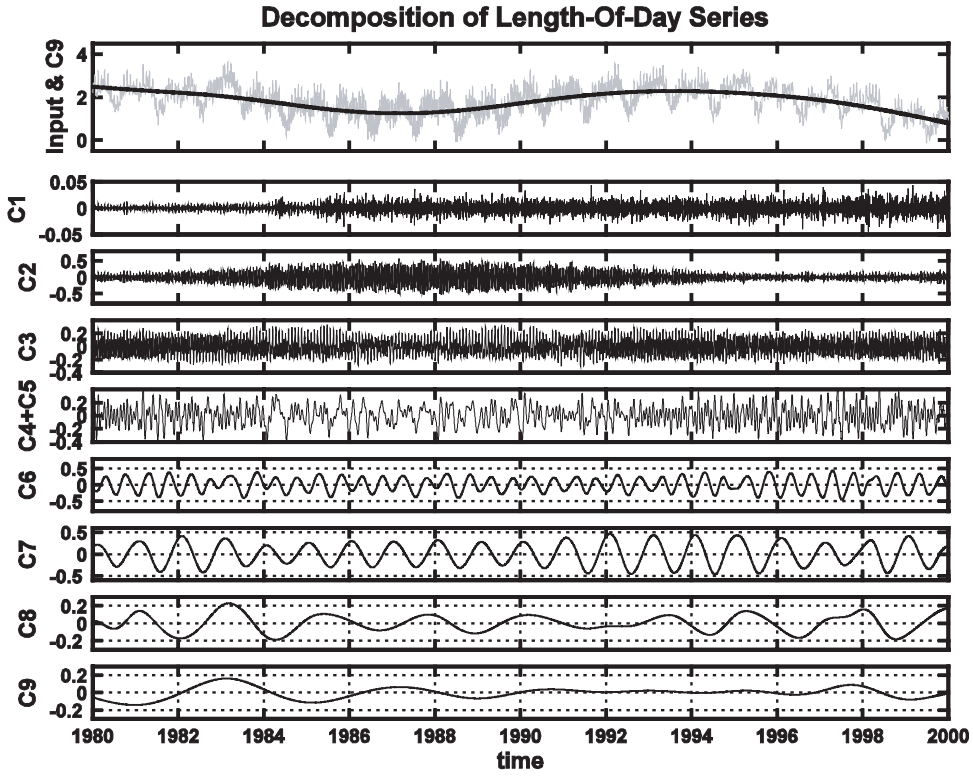

Fig. 20. The EEMD components of the LOD data (the gray line in the top panel) from 1 Jan 1980 to 31 Dec 1999. In the decomposition, noise of standard deviation 0.2 (absolute value, not relative as in the case displayed in the previous figure) is added for the ensemble calculation, and the ensemble number is 800.

propose an EEMD post-processing method using EMD. Figures 20 and 21 provide such an example.

The data used in this example is the Length-of-Day (LOD) data. The LOD was previously analyzed using HHT and studied by Huang *et al.*[39] extensively. In that study, an intermittency test was performed to properly separate oscillations of different timescale when EMD is used to decompose the data. Here, we decompose it using EEMD instead of EMD. The LOD data being decomposed here is from 1 Jan 1980 to 31 Dec 1999. LOD (or part of it) has previously been studied by many researchers.[40–44] Many problems associated with the previous analysis methods were discussed by Huang and Wu,[45] and the locality and adaptivity of EMD/EEMD overcome the drawbacks described above.

The LOD data and its EEMD decomposition are displayed in Fig. 20. In this figure, nine EEMD components (C1 to C9, with C4 and C5 combined), as well as the low-frequency component are displayed over the LOD data, as discussed by Huang and Wu (2008).

The first component, C1, has an averaged amplitude of one order smaller than any other components. It has quasi-regular spikes with an average period around 7 days superimposed on random high-frequency oscillations. These random high-frequency oscillations may be related to weather storms.[39] The second component, C2, has an averaged period about 14 days, which was linked to semi-monthly tides.[39] C3 has an averaged period of about 28 days, which was linked to monthly tides. The combined component, C4+C5, is a component with periods between a month and one-half years. C5 and C6 are semi-annual and annual components, respectively. The causes of these cycles in LOD have been attributed to both the semi-annual and annual cycles of the atmospheric circulation and to other factors, such as tidal strength change related to the revolution of the Earth around the Sun.[43] The next two components are the variations between inter-annual timescales. C7 is quasi-biannual, and C8 has an averaged period slightly larger than 4 years.

Careful examination of these components leads to the conclusion that these components are not IMFs, and therefore, not suitable for Hilbert spectrum analysis. To overcome this drawback, the direct output of the decomposition has been reprocessed with the combination of its components and additional EMD calculation. Since the scale mixing is often caused by high-frequency intermittence, a general approach is to apply EMD to a combination of consecutive components (e.g., D_i and D_{i+1}; for easier description, we here use D instead of C to represent a component of direct EEMD results), extract one IMF which is C_i, and add the remainder ($R_{i,i+1}$) to the next component (D_{i+2}). The sum of the remainder and the next component is subjected to EMD again. Such a process is carried out consecutively.

For our example, the results of this process are displayed in Fig. 21. C1 in Fig. 21 is D1 in Fig. 20; C2 in Fig. 21 is the first mode of the combination of D2 and D3 of Fig. 20 subjected to additional EMD; the difference (D2+D2−C2) is added to D4 of Fig. 20, and the sum is subject to an additional EMD to obtain new C3 of Fig. 21. The leftover in this decomposition is added to D5 and D6. This latter sum is decomposed using an additional EMD to obtain C4 and C5. The sum of D7, D8, and D9 is decomposed using an additional EMD to obtain C6, C7, and C8. The remainder of the LOD data is displayed as the bold line in the top panel.

This reprocess not only corrects the non-IMF problem of EEMD, but also leads to new insights into the characteristics of components, as discussed by Huang and Wu.[45] For example, the amplitude of C2 in Fig. 21 has small semi-annual modulation superimposed on a 19-year modulation. The 19-year modulation is believed to be related to the Metonic cycle. The amplitude of C3 amplitude appears to be relatively small in El Niño years. The systematic phase-locking of C8 of Fig. 21 to El Niño phenomenon was also revealed.

It should be pointed out here that the post-processing process discussed above only provides one choice. While it may improve the result, especially when a particular component is focused, the post-processing may not provide a complete solution to every case for everyone.

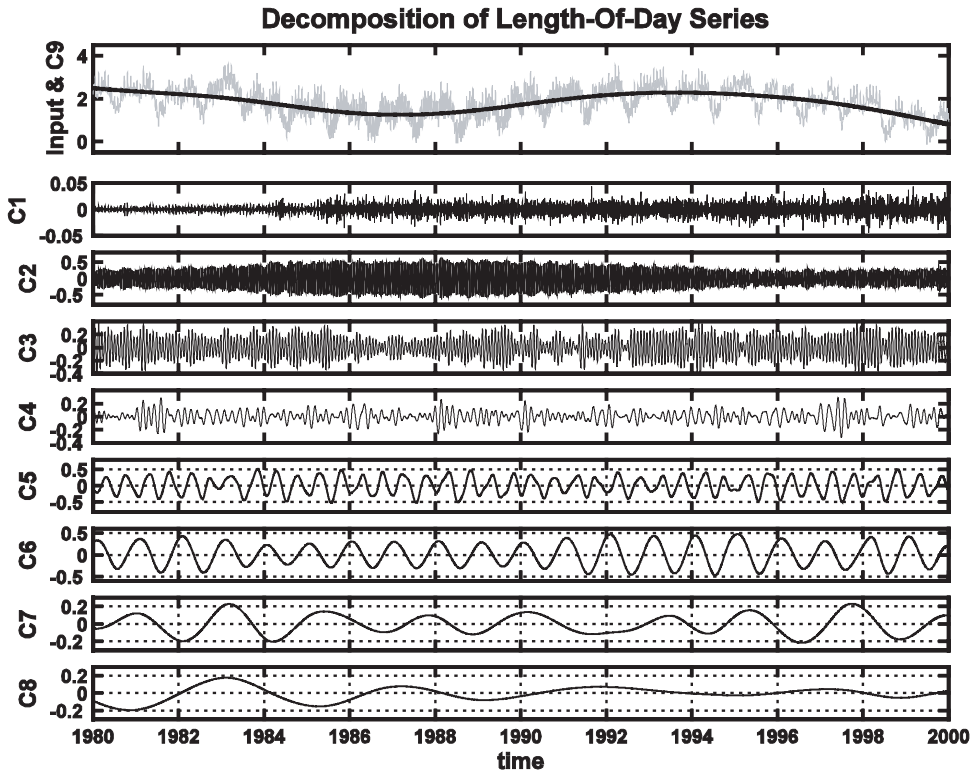

Fig. 21. The reprocessed EEMD components of the LOD data.

6. Discussion and Conclusions

The basic principle of the EEMD is simple; yet, the power of this new approach is obvious from the examples. The new method indeed can separate signals of different scales without undue mode mixing. Adding white noise helps to establish a dyadic reference frame in the time–frequency or timescale space. The real data with a comparable scale can find a natural location to reside. The EEMD utilizes all the statistical characteristic of the noise: it helps to perturb the signal and enable the EMD algorithm to visit all possible solutions in the finite (not infinitesimal) neighborhood of the true final answer; it also takes advantage of the zero mean of the noise to cancel out this noise background once it has served its function of providing the uniformly distributed frame of scales, a feat only possible in the time-domain data analysis. In a way, this new approach is essentially a controlled repeated experiment to produce an ensemble mean for a nonstationary data as the final answer. Since the role of the added noise in the EEMD is to facilitate the separation of different scales of the input data without a real contribution to the IMFs of the data, the EEMD is truly a NADA method that is effective in extracting signals from the data.

Although the noise-added analysis has been tried by the pioneers such as Flandrin *et al.*[5] and Gledhill,[8] there are crucial differences between our approach and theirs. First, both Flandrin and Gledhill define the truth either as the results without noise added, or as given in Eq. (2), which is the limit when the noise-introduced perturbation approaches zero. The truth defined by EEMD is given by the number in the ensemble approaching infinity, i.e.,

$$c_j(t) = \lim_{N\to\infty} \frac{1}{N} \sum_{k=1}^{N} \{c_j(t) + \alpha r_k(t)\}, \tag{7}$$

in which

$$c_j(t) + \alpha r_k(t) \tag{8}$$

is the kth trial of the jth IMF in the noise-added signal, and the magnitude of the added noise, α, is not necessarily small. But, the number of trials in the ensemble, N, has to be large. The difference between the truth and the result of the ensemble is governed by the well-known statistical rule: it decreases as one over the square-root of N, as given in Eq. (6).

With the truth defined, the discrepancy, Δ, instead of the one given in Eq. (3), should be

$$\Delta = \sum_{j=1}^{m} \left(\sum_{t} (E\{cn_j(t)\} - cn_j(t))^2 \right)^{1/2}, \tag{9}$$

in which $E\{\ \}$ is the expected value as given in Eq. (7).

It is proposed here that the EEMD indeed represents a major improvement over the original EMD. As the level of added noise is not of critical importance, as long as it is of finite amplitude to enable a fair ensemble of all the possibilities, the EEMD can be used without any subjective intervention; thus, it provides a truly adaptive data analysis method. By eliminating the problem of mode mixing, it also produces a set of IMFs that bears the full physical meaning, and a time–frequency distribution without transitional gaps. The EMD, with the ensemble approach, has become a more mature tool for nonlinear and nonstationary time series (and other one-dimensional data) analysis.

While the EEMD offers great improvement over the original EMD, there are still some unsettled problems. The first one is a drawback of the EEMD: the EEMD-produced results do not satisfy the strict definition of IMF. Although each trial in the ensemble produces a set of IMF components, the sum of IMF is not necessarily an IMF. The deviations from strict IMFs, however, are small for the examples presented in this study, and have not interfered noticeably in the computation of instantaneous frequency using Hilbert Transform or any other methods, as discussed by Huang *et al.*[3] Nevertheless, these imperfections should be eliminated. One possible solution is to conduct another round of sifting on the IMFs produced by the EEMD. As the IMFs results from the EEMD are of comparable scales, mode mixing would not be a critical problem here, and a simple sift could separate

the riding waves without any problem. This topic will be discussed and reported elsewhere.

The second problem associated with the EEMD is how to treat multi-mode distribution of the IMFs. As discussed by Gledhill,[8] the discrepancy between a trial and its reference tends to show a bimodal (if not multi-modal) distribution. Whenever a bimodal distribution occurs, the discrepancy values could be quite large and the variance value would no longer follow the formula given by Eq. (6). Although part of the large discrepancy could be possibly attributed to the selection of reference as the unperturbed state, the selection of the reference alone cannot explain all the variance and its distribution. The true cause of the problem may be explained easily based on the study of white noise using the EMD by Wu and Huang,[6] in which the dyadic filter bank shows some overlap in scales. Signals having a scale located in the overlapping region would have a finite probability appearing in two different modes. Although the problem has not been fully resolved by far, some alternative implementations of the sifting procedures can alleviate its severity. The first alternative is to tune the noise level and use more trials to reduce the root-mean-squared deviation. Gledhill's results clearly show that this is possible, for the "bimodal" distribution indeed tends to merge into a single, albeit wider, unimodal distribution. The second alternative is the one used in majority cases in this study: sift a low but fixed number of times (10 in this study and discussed in App. A) for obtaining each IMF components. Constrained by the dyadic filter bank property of EMD, this method would almost guarantee the same number of IMFs being sifted out from each trial in the ensemble although the copies of added noise in various trials are different. Both approaches have been tried in this study, but none avoids the multi-mode problem totally. The true solution may have to combine the multi-mode into a single mode, and sift it again to produce a proper single IMF. The third approach is to use rigorous check of each component against the definition, and divide the outcome into different groups according to the total number of IMFs generated. Our experience is that the distribution of the number of IMFs is quite narrow even with a moderate amount of noise perturbation. Then, the peak of the distribution is adopted as the answer. We found all the approaches acceptable, and their differences small. Further studies will be carried out on this issue.

Finally, our experience in using the EEMD brought up two other previously persisted problems for the EMD: the end effect and the stoppage criteria. Both the problems and their solutions are discussed in App. A of this paper. The confidence limit of the EMD-produced results have been addressed to some extent by Huang *et al.*[39] Here the EEMD provides an alternative, yet better, measure of confidence limit, since the EEMD-produced decompositions are much less sensitive to the stoppage criteria used and to the perturbations to data. As for the end effect, the noise-added processes help to ameliorate the difficulty, for with the added noise the end slope will be more uniformly distributed. Thus, the final results could avoid a deterministic drift in one direction or the other.

Acknowledgments

The authors would like to thank Dr P. Flandrin of Ecole Normale Supérieure de Lyon and Dr R. J. Gledhill of Southhampton University for providing their unpublished manuscripts and thesis to us, and Dr S. R. Long of NASA/GSFC Wallops Flight Facility for his careful reading of the early version of the manuscript and comments. Wu is grateful to Drs E. K. Schneider, B. P. Kirtman, and J. L. Kinter of George Mason University and the Center for Ocean–Land–Atmosphere Studies for their helpful suggestions and encouragements. Z. Wu is supported by National Science Foundation of USA under grants ATM-0342104 and ATM-0653136. N. E. Huang is supported in part by a Chair at NCU endowed by Taiwan Semiconductor Manufacturing Company, Ltd., and a grant, NSC 95-2119-M-008-031-MY3, from the National Research Council, Taiwan, ROC.

Appendix A: A Few Algorithm Issues of EMD

As is mentioned earlier, the EMD method has many unsettled issues. Among them, the scale-mixing problem, the selection of a sifting stoppage criterion, and the reduction of end effect are the most concerned ones. With EEMD, the scale-mixing problem is alleviated and the physical uniqueness of the decomposition, to a large degree, is provided, although the complete settlement of the scale-mixing problem is still out of reach. However, the problems of the selection of a sifting stoppage criterion and of the end problem remain open. In this Appendix, we will propose some solutions to these two problems.

A.1. *Local stoppage criteria*

By far, commonly seen stoppage criteria include (1) A Cauchy-type criterion[1] and its variations (e.g., Shen *et al.*[46]); (2) An S-number criterion[39]; (3) A combined global–local stoppage criterion.[47] These criteria have been implemented in various EMD algorithms and tested with a variety of data. Unfortunately, a common undesired feature that these criteria lead to is that the decomposition is sensitive to the local perturbation and to the addition of new data. An example is given in Fig. A.1, in which two time series with some difference at the beginning of the data are decomposed. The stoppage criterion for the sifting used in these decompositions is a modified Cauchy-type criterion, i.e.,

$$C_r = \frac{\sum_i m_{ij}^2}{\sum_i h_{ij}^2}, \tag{A.1}$$

where h_{ij} is the prototype jth IMF after i rounds of sifting, and m_{ij} is the mean of the upper and lower envelopes of h_{ij}. In the decompositions, a value of 0.0001 was selected for C_r.

It is clear that the decompositions are dramatically different. Moreover, the difference seems not to appear in a way that it can be considered as a gradual propagation away from the original difference from the source area. Rather, it appears

Table A.1. The actual sifting numbers in the decompositions to obtain an individual IMF.

	The first time series (bold gray)	The second time series (thin black)
IMF #1	18	17
IMF #2	36	1125
IMF #3	26	22

quite irregularly over the whole temporal domain, starting from the second IMF. This drawback is certainly against the perception that EMD is a local analysis method, and also causes difficulty in the interpretation of the physical meaning of individual IMF. What is going on in the two decompositions?

The answer to the question is rooted deeply in the sifting and its stoppage criterion. To illustrate that point, the actual sifting numbers in the decompositions of these two time series are investigated. Table A.1 gives the sifting numbers for both decompositions. Since the stoppage criterion used in the decompositions contains summations over the global domain, a local change in a prototype IMF may result in a different actual sifting number to obtain the corresponding IMF. That is indeed the case for the two decompositions. As shown in Table A.1, the actual sifting numbers are dramatically different. The increment of the sifting number can result in new local extrema if the prototype IMF contains "wiggles" locally and new high-frequency oscillations appear. That is indeed the case occurring in the decomposition of the second time series (thin-black), for example, the high-frequency oscillations near data point 100 of the second IMF of the second time series, causing new type of scale mixing. Such a process is the main source of the "nonlocal effect" in the EMD sifting. Due to the limitation of length, more detailed discussion will be provided elsewhere.

To eliminate this unpleasant effect of extra sifting, the solution is to use local stoppage criteria. However, to design a universally well-suited local criterion based on the spirits of previously mentioned criteria seems not likely. For this reason, Wu and Huang,[6] proposed to fix the sifting number for the decomposition. Since the spline fitting to obtain the local envelope using only local extrema information, it is expected that the remote effect is negligibly small when the same local process (sifting) is applied to identical data. Indeed, this point can be easily demonstrated through the decomposition of the same two time series in Fig. A.1, which is plotted in Fig. A.2. Clearly, when the sifting number is fixed to 10, the decompositions of two times are almost exactly the same outside the area in which the original data have a difference.

The final question is what should be the optimal number. Our systematic study of that problem shows that a number about 10 would lead to EMD being an almost perfect dyadic filter for noise while keeping the upper and lower envelopes of IMFs almost symmetric with respect to the zero line. That study also leads to a major conjecture about the properties of EMD that EMD can be a filter of any ratio from

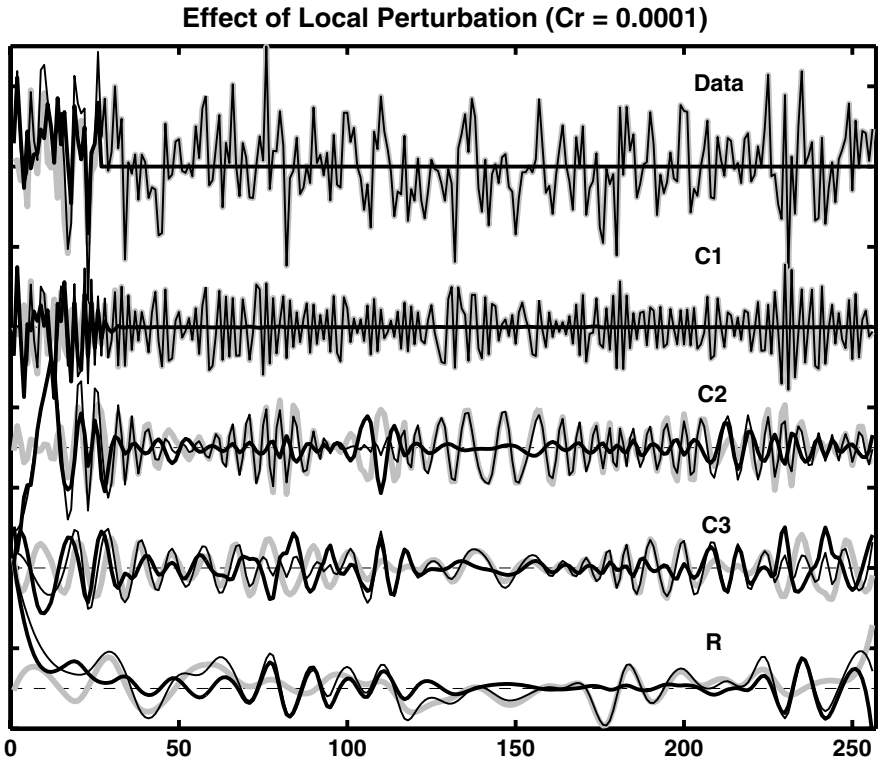

Fig. A.1. The EMD decompositions of two time series with difference in the first 10% of data. The original data of the first and second time series and their components are plotted as the bold-gray and thin-black lines, respectively. The bold-black lines are the difference of two original time series or of the corresponding individual IMFs.

1 to 2, which reveals the relationships of EMD with the Fourier transform and with the wavelet analysis. The detailed report of that study will be published later in a separate paper.

A.2. *An ensemble approach to reduce end effects*

End effects have caused problems to all known data analysis methods in the calculation processes and in the interpretation of the results. Traditionally, there are two types of thinking to deal with end effects. The first type is to analyze data of a given length directly, but to interpret the results cautiously by determining the windows within which the analysis is reliable. The determination of reliable windows is often analysis-method-related but not related to data itself, leading to throwing away some precious information contained in data near the ends. This thinking has been often applied to analyze data in Fourier analysis by using various windows and continuous wavelet analyses. The second thinking is to extend data implicitly or explicitly beyond the existing range as proposed by Huang *et al.*[1] For

example, the Fourier transform, although applied only to the existing data range, has an implicit assumption that the data of the existing range will repeat piecewise. Other methods, such as neural networks, assume that some characteristics of the existing data will hold in the future evolution of the system and devise a predicting model to extend the data. All these approaches have demonstrated their usefulness in particular examples. However, due to various rigid stationary and linear assumptions, these thinking can hardly deal well with the nonlinear nonstationary data.

For EMD, the method of extending data beyond the existing range has been often adopted so as to carry out the spline envelope fitting over and even beyond the existing data range; otherwise, we have to stop the spline at the last extremum. To achieve the goal of extension of data, numerous methods, such as the linear prediction, mirror or anti-mirror extension, neural networks, and vector machines, to name a few, have been used. While methods for extending data vary, the essence of all these methods is to predict data, a dauntingly difficult procedure even for linear and stationary processes. The problem that must be faced is how to make predictions for nonlinear and nonstationary stochastic processes. To bypass difficulties in data extension, new approach to alleviate end effects is in urgent demand.

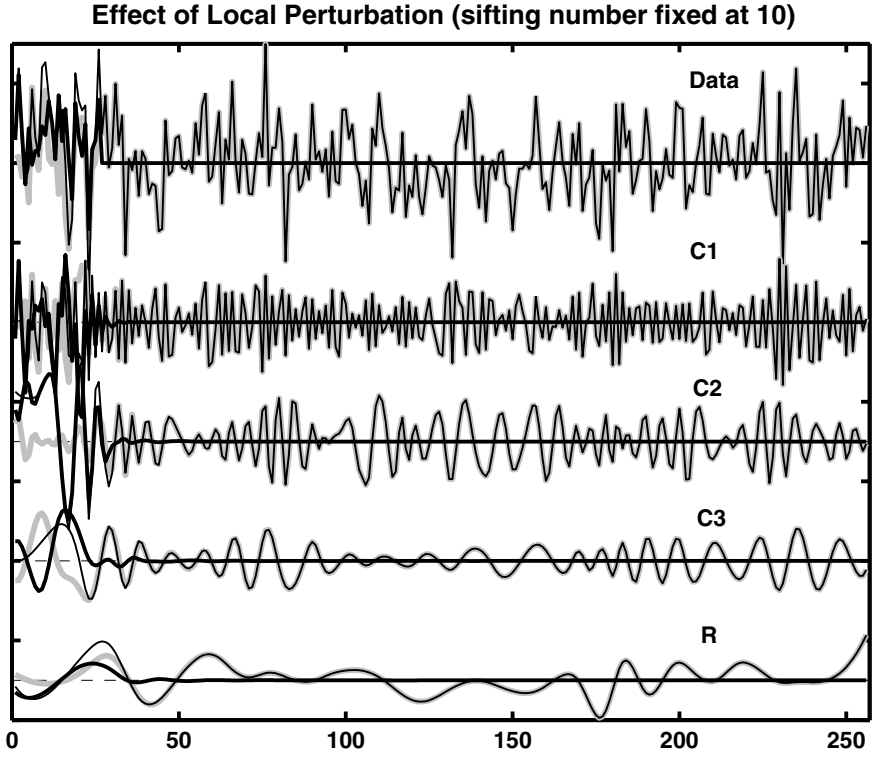

Fig. A.2. Same as in Fig. A.1, but with a fixed sifting number 10.

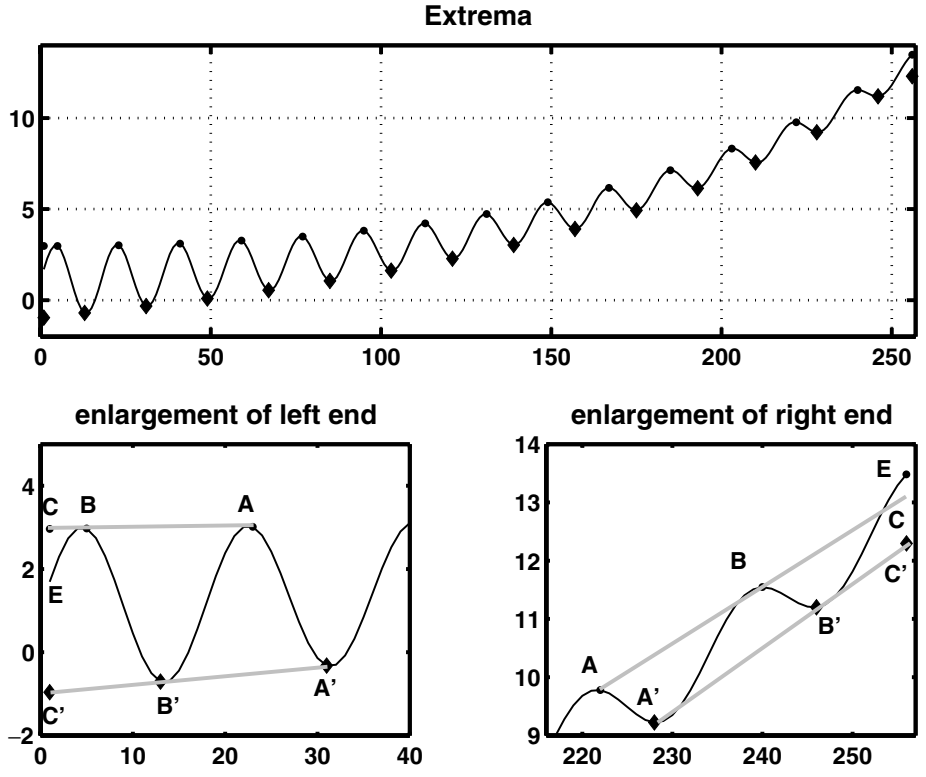

Fig. A.3. A method to reduce the end effects of EMD. In the upper panel, the black line is the schematic signal, and the dots (diamonds) are the maxima (minima) for the upper (lower) envelope fitting. The lower left (right) panel is an enlargement of the left (right) end of the upper panel. The upper (lower) gray line is the extended straight line that connects the last two maxima (minima) near a data end.

The thinking behind our new approach was outlined by Huang and Wu,[45] in which they proposed that the necessary information needed to carry out the EMD sifting is two values at the two ends of any prototype IMF, and to obtain that information may not involve necessarily the prediction of data. This new thinking is indeed the guideline for the following general method to reduce end effects.

The method is schematically presented in Fig. A.3. Suppose we have a signal as plotted in black line in the upper panel. For such a signal, the interior extrema are easily identified. However, these extrema are not enough to determine two well-behaved fitting spline envelopes near the two ends for the sifting, especially in the cases when the total number of splines are small, for the extrapolation of a spline often leads to undesirable big error especially near the ends. Unfortunately, the end error may propagate from the ends to the interior of the data span that would cause severe deterioration of the IMFs obtained. To avoid this problem, we devise a method to determine a maximum and a minimum at the end of a prototype IMF.

The method is schematically illustrated in the lower panels of Fig. A.1. Suppose that we have two maxima A and B that are closest to an end, we linearly extend straight line AB to the end to find C. If C is larger than the end-point value E of the prototype IMF, we consider C as a new maximum for the upper spline envelope fitting (the case corresponding to the lower left panel of Fig. A.1), otherwise, we consider E as a new maximum for the upper spline envelope fitting (the case corresponding to the lower right panel of Fig. A.1). Similarly, we determine the end point for the lower envelope fitting. In the cases when one only have one or no interior maximum (minimum), the two ends of the prototype IMF are assigned as two maxima (minima) for both the upper and lower envelope fittings, using either the second-order polynomial or the linear fitting, respectively.

The above proposed method is simple but has behaved well in analyzing numerous time series of dramatically different characteristics. However, when the targeted time series ends with strangely behaved data, the end effect could still be noticeable. However, the sensitivity to the strangely behaved data at the end of the targeted time series is significantly reduced when this end approach is applied with EEMD. Such a property is very important to obtain accurately the useful information in data, especially in finding trend and detrending.[48]

It should be noted here that the reason to use linear extrapolation rather than higher order polynomial extrapolation is (1) to keep the locality of the EMD, for linear extrapolation needs only two maxima (minima) near an end; and (2) the higher order polynomial extrapolation tends to lead to large deviations from visually acceptable range of possible envelope ending at an end when it is used with EEMD.

Appendix B: A Matlab EMD/EEMD Code Package

During the past decade, EMD has become a tool of choice in many scientific and engineering fields. While many users have developed by themselves EMD programs in various computational languages for their own usage, there are also a few web-accessible programs. Among them, the most influential two are produced by the Goddard Space Flight Center (http://tco.gsfc.nasa.gov/hht/) and by Flandrin's group (http://perso.ens-lyon.fr/patrick.flandrin/emd.html), which have served many users in their research using EMD. However, many of recent developments of EMD have not been integrated into these software.

To further facilitate researchers from various scientific and engineering fields to use EMD in their studies, we provide an alternative package of Matlab EMD/EEMD program that can be easily used. The program integrates most of our recent developments of EMD, such as those discussed in this paper, and it includes the following components:

1. The basic EMD/EEMD program;
2. The statistical significance test of IMFs; and
3. An EMD-based instantaneous frequency calculation method.

The program and its instructions can be downloaded from http://rcada.ncu.edu.tw/

References

1. N. E. Huang, Z. Shen, S. R. Long, M. C. Wu, E. H. Shih, Q. Zheng, C. C. Tung and H. H. Liu, The empirical mode decomposition method and the Hilbert spectrum for non-stationary time series analysis, *Proc. Roy. Soc. London* **454A** (1998) 903–995.
2. N. E. Huang, Z. Shen and R. S. Long, A new view of nonlinear water waves — the Hilbert spectrum, *Ann. Rev. Fluid Mech.* **31** (1999) 417–457.
3. N. E. Huang and S. S. P. Shen (ed.), *Hilbert–Huang Transform and Its Applications* (World Scientific, Singapore, 2005), p. 311.
4. N. E. Huang and N. O. Attoh-Okine (ed.), *Hilbert–Huang Transform in Engineering* (CRC Press, 2005), p. 313.
5. P. Flandrin, G. Rilling and P. Gonçalvès, Empirical mode decomposition as a filter bank, *IEEE Signal Process. Lett.* **11** (2004) 112–114.
6. Z. Wu and N. E. Huang, A study of the characteristics of white noise using the empirical mode decomposition method, *Proc. Roy. Soc. London* **460A** (2004) 1597–1611.
7. P. Flandrin, P. Gonçalvès and G. Rilling, EMD equivalent filter banks, from interpretation to applications, in *Hilbert–Huang Transform: Introduction and Applications*, eds. N. E. Huang and S. S. P. Shen (World Scientific, Singapore, 2005), pp. 67–87.
8. R. J. Gledhill, Methods for investigating conformational change in biomolecular simulations, A dissertation for the degree of Doctor of Philosophy at the Department of Chemistry, the University of Southampton (2003), p. 201.
9. Z. Wu and N. E. Huang, Statistical significant test of intrinsic mode functions, in *Hilbert–Huang Transform: Introduction and Applications*, eds. N. E. Huang and S. S. P. Shen (World Scientific, Singapore, 2005), pp. 125–148.
10. H. Press and J. W. Tukey, Power spectral methods of analysis and their application to problems in airplane dynamics, *Bell System Monograph* (1956) #2606.
11. H. Fuenzalida and B. Rosenbluth, Prewhitening of climatological time-series, *J. Climate* **3** (1990) 382–393.
12. M. J. Link and K. M. Buckley, Prewhitening for intelligibility gain in hearing-aid arrays, *J. Acoust. Soc. Am.* **93** (1993) 2139–2145.
13. C. A. Zala, J. M. Ozard and M. J. Wilmut, Prewhitening for improved detection by matched-field processing in ice-ridging correlated noise, *J. Acoust. Soc. Am.* **98**(5) (1995) 2726–2734.
14. R. N. Strickland and H. IlHahn, Wavelet transform methods for object detection and recovery, *IEEE Trans. Image Proc.* **6** (1997) 724–735.
15. A. Trucco, Experimental results on the detection of embedded objects by a prewhitening filter, *IEEE J. Ocean. Eng.* **26** (2001) 783–794.
16. M. B. Priestley, *Spectral Analysis and Time Series* (Academic Press, London, 1991), p. 890.
17. C. S. Kao, A. C. Tamhane and R. S. H. Mah, A general prewhitening procedure for process and measurement noises, *Chem. Eng. Comm.* **118** (1992) 49–57.
18. D. N. Politis, Arma models, prewhitening, and minimum cross entropy, *IEEE Trans. Signal Process.* **41** (1993) 781–787.
19. S. C. Douglas, A. Cichocki and S. Amari, Self-whitening algorithms for adaptive equalization and deconvolution, *IEEE Trans. Signal Process.* **47** (1999) 1161–1165.
20. A. Cichocki and S. Amari, *Adaptive Blind Signal and Image Processing* (John Wiley, Chichester, UK, 2002), p. 464.
21. L. De Lathauwer, B. De Moor and J. Vandewalle, A prewhitening-induced bound on the identification error in independent component analysis, *IEEE Trans. Circuits Syst. I-Regular Papers* **52** (2005) 546–554.

22. L. Gammaitoni, P. Hanggi, P. Jung and F. Marchesoni, Stochastic resonance, *Rev. Mod. Phys.* **70** (1998) 223–288.
23. N. E. Huang, C. C. Chern, K. Huang, L. Salvino, S. R. Long and K. L. Fan, Spectral analysis of the Chi-Chi earthquake data: Station TUC129, Taiwan, September 21, *Bull. Seismol. Soc. Am.* **91** (2001) 1310–1338.
24. S. G. Philander, *El Niño, La Niña, and the Southern Oscillations* (Academic Press, 1990), p. 293.
25. National Research Council, *Learning to Predict Climate Variations Associated with El Niño and the Southern Oscillation* (National Academy Press, 1996), p. 171.
26. M. H. Glantz, R. W. Katz and N. Nicholls (eds.), *Teleconnections Linking Worldwide Climate Anomalies* (Cambridge University Press, 1991), p. 535.
27. M. J. Suarez and P. S. Schopf, A delayed action oscillator for ENSO, *J. Atmos. Sci.* **45** (1988) 3283–3287.
28. D. S. Battisti and A. C. Hirst, Interannual variability in a tropical atmosphere ocean model: Influence of the basic state, ocean geometry and nonlinearity, *J. Atmos. Sci.* **46** (1989) 1687–1712.
29. F.-F. Jin, Tropical ocean–atmosphere interaction, the Pacific cold tongue, and the El Niño-Southern oscillation, *Science* **274** (1996) 76–78.
30. K. E. Trenberth, Signal versus noise in the southern oscillation, *Monthly Weather Rev.* **112** (1984) 326–332.
31. C. Deser and J. M. Wallace, Large-scale atmospheric circulation features of warm and cold episodes in the tropical Pacific, *J. Climate* **3** (1990) 1254–1281.
32. Z. Wu, E. K. Schneider, Z. Z. Hu and L. Cao, The impact of global warming on ENSO variability in climate records, COLA Technical Report (2001) CTR 110.
33. M. Ghil, M. R. Allen, M. D. Dettinger, K. Ide, D. Kondrashov, M. E. Mann, A. W. Robertson, A. Saunders, Y. Tian, F. Varadi and P. Yiou, Advanced spectral methods for climatic time series, *Rev. Geophys.* **40** (2002) 10.1029/2000GR000092.
34. C. F. Ropelewski and P. D. Jones, An extension of the Tahiti-Darwin southern oscillation index, *Monthly Weather Rev.* **115** (1987) 2161–2165.
35. R. J. Allan, N. Nicholls, P. D. Jones and I. J. Butterworth, A further extension of the Tahiti-Darwin SOI, early ENSO events and Darwin pressure, *J. Climate* **4** (1991) 743–749.
36. N. A. Rayner, E. B. Holton, D. E. Parker, C. K. Folland and R. B. Hackett, *Global Sea-Ice and Sea Surface Temperature Data Set, 1903–1994. Version 2.2*, Hadley Center for Climate Prediction and Research Tech. Note 74, Met Office, Bracknell, Berkshire, United Kingdom.
37. S.-W. Yeh and B. P. Kirtman, Tropical Pacific decadal variability and ENSO amplitude modulation in a CGCM, COLA Technical Report (2004) CTR 164.
38. N. E. Huang, Empirical mode decomposition for analyzing acoustic signal, US Patent 10-073857, August (2003), Pending.
39. N. E. Huang, M. L. Wu, S. R. Long, S. S. Shen, W. D. Qu, P. Gloersen and K. L. Fan, A confidence limit for the empirical mode decomposition and the Hilbert spectral analysis, *Proc. Roy. Soc. London* **459A** (2003) 2317–2345.
40. R. T. H. Barnes, R. Hide, A. A. White and C. A. Wilson, Atmospheric angular momentum fluctuations, length-of-day changes and polar motion, *Proc. Roy. Soc. London* **387A** (1983) 31–73.
41. R. D. Rosen and D. A. Salstein, Variations in atmospheric angular momentum on global and regional scales and the length of day, *J. Geophys. Res.* **88** (1983) 5451–5470.

42. B. F. Chao, Length-of-day variations caused by El Niño-southern oscillation and quasi-biennial oscillation, *Science* **243** (1989) 923–925.
43. J. Höpfner, Seasonal variations in length of day and atmospheric angular momentum, *Geophys. J. Int.* **135** (1998) 407–437.
44. H. Razmi, On the tidal force of the Moon on the Earth, *Eur. J. Phys.* **26** (2005) 927–934.
45. N. E. Huang and Z. Wu, A review on Hilbert–Huang transform: the method and its applications on geophysical studies, *Rev. Geophys.* **46** (2008), RG 2006, doi: 10.1029/2007RG000228.
46. S. P. Shen, T. Shu, N. E. Huang, Z. Wu, G. R. North, T. R. Carl and D. R. Easterling, HHT analysis of the nonlinear and non-stationary annual cycle of daily surface air temperature data, in *Hibert-Huang Transform: Introduction and Application*, pp. 187–210, ed. N. E. Huang and S. S. P. Shen (World scientific, Singapore, 2005), pp. 311
47. G. Rilling, P. Flandrin and P. Goncalvés: On empirical mode decomposition and its algorithms, *IEEE-EURASIP workshop on Nonlinear Signal and Image Processing NSIP-03*, Grado(I), 2003.
48. Z. Wu, N. E. Huang, S. R. Long and C.-K. Peng, On the trend, detrending, and the variability of nonlinear and non-stationary time series, *Proc. Natl. Acad. Sci. USA* **104** (2007) 14889–14894

This article has been cited by:

1. Zhipeng Feng, Ming Liang, Fulei Chu. 2013. Recent advances in time–frequency analysis methods for machinery fault diagnosis: A review with application examples. *Mechanical Systems and Signal Processing* **38**:1, 165-205. [CrossRef]
2. A. Rojas, J.M. Górriz, J. Ramírez, I.A. Illán, F.J. Martínez-Murcia, A. Ortiz, M. Gómez Río, M. Moreno-Caballero. 2013. Application of Empirical Mode Decomposition (EMD) on DaTSCAN SPECT images to explore Parkinson Disease. *Expert Systems with Applications* **40**:7, 2756-2766. [CrossRef]
3. Qing Zhao, Wei Gao, Weining Xiang, Runhe Shi, Chaoshun Liu, Tianyong Zhai, Hung-lung Allen Huang, Liam E. Gumley, Kathleen Strabala. 2013. Analysis of air quality variability in Shanghai using AOD and API data in the recent decade. *Frontiers of Earth Science* **7**:2, 159-168. [CrossRef]
4. Yi Zhou, Sheng-Tong Zhou, Zuo-Yang Zhong, Hong-Guang Li. 2013. A de-illumination scheme for face recognition based on fast decomposition and detail feature fusion. *Optics Express* **21**:9, 11294. [CrossRef]
5. M. Amarnath, I.R. Praveen Krishna. 2013. Detection and diagnosis of surface wear failure in a spur geared system using EEMD based vibration signalanalysis. *Tribology International* **61**, 224-234. [CrossRef]
6. Shaopeng Liu, Robert X. Gao, Dinesh John, John Staudenmayer, Patty Freedson. 2013. Tissue Artifact Removal from Respiratory Signals Based on Empirical Mode Decomposition. *Annals of Biomedical Engineering* **41**:5, 1003-1015. [CrossRef]
7. Jiesi Luo, Dejie Yu, Ming Liang. 2013. A kurtosis-guided adaptive demodulation technique for bearing fault detection based on tunable-Q wavelet transform. *Measurement Science and Technology* **24**:5, 055009. [CrossRef]
8. Xianyao Chen, Meng Wang, Yuanling Zhang, Ying Feng, Zhaohua Wu, Norden E. Huang. 2013. Detecting Signals from Data with Noise: Theory and Applications. *Journal of the Atmospheric Sciences* **70**:5, 1489-1504. [CrossRef]
9. Yanli Yang, Changyun Miao, Jiahao Deng. 2013. An Analytical Expression for Empirical Mode Decomposition Based on B-Spline Interpolation. *Circuits, Systems, and Signal Processing* . [CrossRef]
10. Ying Zhang, Hongfu Zuo, Fang Bai. 2013. Classification of fault location and performance degradation of a roller bearing. *Measurement* **46**:3, 1178-1189. [CrossRef]
11. Xu Zhang, Ping Zhou. 2013. Filtering of surface EMG using ensemble empirical mode decomposition. *Medical Engineering & Physics* **35**:4, 537-542. [CrossRef]
12. Rahul Soangra, Thurmon E. Lockhart, John Lach, Emaad M. Abdel-Rahman. 2013. Effects of Hemodialysis Therapy on Sit-to-Walk Characteristics in End Stage Renal Disease Patients. *Annals of Biomedical Engineering* **41**:4, 795-805. [CrossRef]
13. Nehemiah T. Liu, Andriy I. Batchinsky, Leopoldo C. Cancio, William L. Baker, Jose Salinas. 2013. Development and validation of a novel fusion algorithm for continuous, accurate, and automated R-wave detection and calculation of signal-derived metrics. *Journal of Critical Care* . [CrossRef]

14. Hongkai Jiang, Chengliang Li, Huaxing Li. 2013. An improved EEMD with multiwavelet packet for rotating machinery multi-fault diagnosis. *Mechanical Systems and Signal Processing* **36**:2, 225-239. [CrossRef]
15. Peter C. Chu, Chenwu Fan, Norden Huang. 2013. Derivative-optimized empirical mode decomposition for the Hilbert-Huang transform. *Journal of Computational and Applied Mathematics* . [CrossRef]
16. L. J. Wilcox, A. J. Charlton-Perez. 2013. Final warming of the Southern Hemisphere polar vortex in high- and low-top CMIP5 models. *Journal of Geophysical Research: Atmospheres* **118**:6, 2535-2546. [CrossRef]
17. Stelios Krinidis, Michail Krinidis. 2013. Skeletonization based on angle maps. *Pattern Analysis and Applications* . [CrossRef]
18. Kais Khaldi, Abdel-Ouahab Boudraa, Bruno Torresani, Thierry Chonavel. 2013. HHT-based audio coding. *Signal, Image and Video Processing* . [CrossRef]
19. Yi Qin. 2013. Multicomponent AM–FM demodulation based on energy separation and adaptive filtering. *Mechanical Systems and Signal Processing* . [CrossRef]
20. Jinshan Lin, Qian Chen. 2013. Fault diagnosis of rolling bearings based on multifractal detrended fluctuation analysis and Mahalanobis distance criterion. *Mechanical Systems and Signal Processing* . [CrossRef]
21. Chunlin Xia, Yangfang Wu, Qianqian Lu. 2013. Transversal vibration analysis of an axially moving string with unilateral constraints using the HHT method. *Mechanical Systems and Signal Processing* . [CrossRef]
22. Guilherme S. Welter, Paulo A. A. Esquef. 2013. Multifractal analysis based on amplitude extrema of intrinsic mode functions. *Physical Review E* **87**:3. . [CrossRef]
23. Cheng Lian, Zhigang Zeng, Wei Yao, Huiming Tang. 2013. Displacement prediction model of landslide based on a modified ensemble empirical mode decomposition and extreme learning machine. *Natural Hazards* **66**:2, 759-771. [CrossRef]
24. Dan Chen, Dongcuan Lu, Mingwei Tian, Shan He, Shuaiting Wang, Jian Tian, Chang Cai, Xiaoli Li. 2013. Towards energy-efficient parallel analysis of neural signals. *Cluster Computing* **16**:1, 39-53. [CrossRef]
25. Van Tung Tran, Bo-Suk Yang, Fengshou Gu, Andrew Ball. 2013. Thermal image enhancement using bi-dimensional empirical mode decomposition in combination with relevance vector machine for rotating machinery fault diagnosis. *Mechanical Systems and Signal Processing* . [CrossRef]
26. Boqiang Huang, Angela Kunoth. 2013. An optimization based empirical mode decomposition scheme. *Journal of Computational and Applied Mathematics* **240**, 174-183. [CrossRef]
27. Yuan Shi, King-Fai Li, Yuk L. Yung, Hartmut H. Aumann, Zuoqiang Shi, Thomas Y. Hou. 2013. A decadal microwave record of tropical air temperature from AMSU-A/aqua observations. *Climate Dynamics* . [CrossRef]
28. Jiajun Han, Mirko van der Baan. 2013. Empirical mode decomposition for seismic time-frequency analysis. *GEOPHYSICS* **78**:2, O9-O19. [CrossRef]

29. JING WANG, PENGJIAN SHANG, XIAOJUN ZHAO, JIANAN XIA. 2013. MULTISCALE ENTROPY ANALYSIS OF TRAFFIC TIME SERIES. *International Journal of Modern Physics C* **24**:02. . [Abstract] [PDF] [PDF Plus]
30. Yi Zhou, Hongguang Li. 2013. A denoising scheme for DSPI fringes based on fast bi-dimensional ensemble empirical mode decomposition and BIMF energy estimation. *Mechanical Systems and Signal Processing* **35**:1-2, 369-382. [CrossRef]
31. V. Misra, J.-P. Michael. 2013. Varied Diagnosis of the Observed Surface Temperature Trends in the Southeast United States. *Journal of Climate* **26**:4, 1467-1472. [CrossRef]
32. Yaguo Lei, Jing Lin, Zhengjia He, Ming J. Zuo. 2013. A review on empirical mode decomposition in fault diagnosis of rotating machinery. *Mechanical Systems and Signal Processing* **35**:1-2, 108-126. [CrossRef]
33. Okan Ozgonenel, Turgay Yalcin, Irfan Guney, Unal Kurt. 2013. A new classification for power quality events in distribution systems. *Electric Power Systems Research* **95**, 192-199. [CrossRef]
34. A. Zeiler, R. Faltermeier, A. M. Tomé, C. Puntonet, A. Brawanski, E. W. Lang. 2013. Weighted Sliding Empirical Mode Decomposition for Online Analysis of Biomedical Time Series. *Neural Processing Letters* **37**:1, 21-32. [CrossRef]
35. Amir Eftekhar, Christofer Toumazou, Emmanuel M. Drakakis. 2013. Empirical Mode Decomposition: Real-Time Implementation and Applications. *Journal of Signal Processing Systems* . [CrossRef]
36. Zhigang Liu, Wanlu Sun, Jiajun Zeng. 2013. A new short-term load forecasting method of power system based on EEMD and SS-PSO. *Neural Computing and Applications* . [CrossRef]
37. Wei Guo, Peter W. Tse. 2013. A novel signal compression method based on optimal ensemble empirical mode decomposition for bearing vibration signals. *Journal of Sound and Vibration* **332**:2, 423-441. [CrossRef]
38. Chun-Yi Lin, Chung-Ru Ho, Yung-Hsiang Lee, Nan-Jung Kuo, Shin-Jye Liang. 2013. Thermal variability of the Indo-Pacific warm pool. *Global and Planetary Change* **100**, 234-244. [CrossRef]
39. Laurence C. Breaker, Alexander Ruzmaikin. 2013. Estimating Rates of Acceleration Based on the 157-Year Record of Sea Level from San Francisco, California, U.S.A. *Journal of Coastal Research* **286**, 43-51. [CrossRef]
40. CHIH-YU KUO, SHAO-KUAN WEI, PI-WEN TSAI. 2013. ENSEMBLE EMPIRICAL MODE DECOMPOSITION WITH SUPERVISED CLUSTER ANALYSIS. *Advances in Adaptive Data Analysis* **05**:01. . [Citation] [PDF Plus]
41. CHIA-CHI CHANG, HUNG-YI HSU, TZU-CHIEN HSIAO. 2013. QUANTITATIVE NON-STATIONARY ASSESSMENT OF CEREBRAL HEMODYNAMICS BY EMPIRICAL MODE DECOMPOSITION OF CEREBRAL DOPPLER FLOW VELOCITY. *Advances in Adaptive Data Analysis* **05**:01. . [Citation] [PDF Plus]
42. Michael E. Kozar, Vasubandhu Misra. 2012. Evaluation of twentieth-century Atlantic Warm Pool simulations in historical CMIP5 runs. *Climate Dynamics* . [CrossRef]

43. C. Franzke. 2012. On the statistical significance of surface air temperature trends in the Eurasian Arctic region. *Geophysical Research Letters* **39**:23, n/a-n/a. [CrossRef]
44. Huey-Kuo Chen, Che-Jung Wu. 2012. Travel Time Prediction Using Empirical Mode Decomposition and Gray Theory. *Transportation Research Record: Journal of the Transportation Research Board* **2324**:-1, 11-19. [CrossRef]
45. A. Gallix, J.M. Górriz, J. Ramírez, I.A. Illán, E.W. Lang. 2012. On the empirical mode decomposition applied to the analysis of brain SPECT images. *Expert Systems with Applications* **39**:18, 13451-13461. [CrossRef]
46. S. Ramezani, O. Bahar. 2012. EFFICACY OF THE ENHANCED TRANSFORM IN COMPARISON WITH THE CLASSIC HILBERT-HUANG METHOD. *Sharif* **28**:1. . [CrossRef]
47. Yi ZHENG, Xiaofeng SUN, Jian CHEN, Jun YUE. 2012. Extracting pulse signals in measurement while drilling using optimum denoising methods based on the ensemble empirical mode decomposition. *Petroleum Exploration and Development* **39**:6, 798-801. [CrossRef]
48. Suneet Dwivedi. 2012. Forecasting the peak anomalies of dominant intrinsic modes of Indian Ocean Dipole. *Deep Sea Research Part I: Oceanographic Research Papers* **70**, 73-82. [CrossRef]
49. Yina Guo, Shuhua Huang, Yongtang Li. 2012. Single-Mixture Source Separation Using Dimensionality Reduction of Ensemble Empirical Mode Decomposition and Independent Component Analysis. *Circuits, Systems, and Signal Processing* **31**:6, 2047-2060. [CrossRef]
50. J L Kueny, M Lourenco, J L Ballester. 2012. Transient flow analysis linked to fast pressure disturbance monitored in pipe systems. *IOP Conference Series: Earth and Environmental Science* **15**:4, 042021. [CrossRef]
51. Artūras Janušauskas, Vaidotas Marozas, Arūnas Lukoševičius. 2012. Ensemble empirical mode decomposition based feature enhancement of cardio signals. *Medical Engineering & Physics* . [CrossRef]
52. Zhipeng Feng, Ming Liang, Yi Zhang, Shumin Hou. 2012. Fault diagnosis for wind turbine planetary gearboxes via demodulation analysis based on ensemble empirical mode decomposition and energy separation. *Renewable Energy* **47**, 112-126. [CrossRef]
53. Xianyao Chen, Yuanling Zhang, Min Zhang, Ying Feng, Zhaohua Wu, Fangli Qiao, Norden Eh Huang. 2012. Intercomparison between observed and simulated variability in global ocean heat content using empirical mode decomposition, part I: modulated annual cycle. *Climate Dynamics* . [CrossRef]
54. MARCELO A. COLOMINAS, GASTÓN SCHLOTTHAUER, MARÍA E. TORRES, PATRICK FLANDRIN. 2012. NOISE-ASSISTED EMD METHODS IN ACTION. *Advances in Adaptive Data Analysis* **04**:04. . [Citation] [PDF Plus]
55. S. T. G. RAGHUKANTH, S. SANGEETHA. 2012. EMPIRICAL MODE DECOMPOSITION OF EARTHQUAKE ACCELEROGRAMS. *Advances in Adaptive Data Analysis* **04**:04. . [Citation] [PDF Plus]
56. KOSEKI J. KOBAYASHI-KIRSCHVINK, KING-FAI LI, RUN-LIE SHIA, YUK L. YUNG. 2012. FUNDAMENTAL MODES OF ATMOSPHERIC CFC-11 FROM

EMPIRICAL MODE DECOMPOSITION. *Advances in Adaptive Data Analysis* **04**:04. . [Citation] [PDF Plus]

57. Xin Xiong, Shixi Yang, Chunbiao Gan. 2012. A new procedure for extracting fault feature of multi-frequency signal from rotating machinery. *Mechanical Systems and Signal Processing* **32**, 306-319. [CrossRef]
58. Martin Gagnon, Antoine Tahan, Philippe Bocher, Denis Thibault. 2012. On the stochastic simulation of hydroelectric turbine blades transient response. *Mechanical Systems and Signal Processing* **32**, 178-187. [CrossRef]
59. Jian Chen, Ren Zhang, Huizan Wang, Yuzhu An, Peng Peng, Weitao Zhang. 2012. Isolation of sea surface salinity maps on various timescales in the tropical Pacific Ocean. *Journal of Oceanography* **68**:5, 687-701. [CrossRef]
60. Yih Jeng, Chih-Sung Chen. 2012. Subsurface GPR imaging of a potential collapse area in urban environments. *Engineering Geology* **147-148**, 57-67. [CrossRef]
61. Qiang Zhang, Vijay P. Singh, Kun Li, Jianfeng Li. 2012. Trend, periodicity and abrupt change in streamflow of the East River, the Pearl River basin. *Hydrological Processes* n/a-n/a. [CrossRef]
62. Ying Zhang, Zhenhua Xie. 2012. Ensemble empirical mode decomposition of impact-echo data for testing concrete structures. *NDT & E International* **51**, 74-84. [CrossRef]
63. Thomas Y. Hou, Zuoqiang Shi. 2012. Data-driven time–frequency analysis. *Applied and Computational Harmonic Analysis* . [CrossRef]
64. Han Soo Lee, Takao Yamashita, Toyoaki Mishima. 2012. Multi-decadal variations of ENSO, the Pacific Decadal Oscillation and tropical cyclones in the western North Pacific. *Progress in Oceanography* **105**, 67-80. [CrossRef]
65. S. V. Henriksson, P. Räisänen, J. Silén, A. Laaksonen. 2012. Quasiperiodic climate variability with a period of 50–80 years: Fourier analysis of measurements and Earth System Model simulations. *Climate Dynamics* **39**:7-8, 1999-2011. [CrossRef]
66. Z. Qin, X. Zou, F. Weng. 2012. Comparison between linear and nonlinear trends in NOAA-15 AMSU-A brightness temperatures during 1998–2010. *Climate Dynamics* **39**:7-8, 1763-1779. [CrossRef]
67. Yih Jeng, Chu-Lin Huang, Lun-Tao Tong, Ming-Juin Lin, Chih-Sung Chen, Hsin-Han Huang. 2012. Mapping possible subsurface granitic bodies in the northeastern Taiwan mountain belt using the VLF-EM method. *Journal of Applied Geophysics* **85**, 25-36. [CrossRef]
68. Nikolaos Tsakalozos, Konstantinos Drakakis, Scott Rickard. 2012. A formal study of the nonlinearity and consistency of the Empirical Mode Decomposition. *Signal Processing* **92**:9, 1961-1969. [CrossRef]
69. V. Misra, S. M. DiNapoli. 2012. The observed teleconnection between the equatorial Amazon and the Intra-Americas Seas. *Climate Dynamics* . [CrossRef]
70. Matthias Joachim Ehrhardt, H. Villinger, S. Schiffler. 2012. Evaluation of decomposition tools for sea floor pressure data. *Computers & Geosciences* **45**, 4-12. [CrossRef]

71. Bohua Huang, Zeng-Zhen Hu, Edwin K. Schneider, Zhaohua Wu, Yan Xue, Barry Klinger. 2012. Influences of tropical–extratropical interaction on the multidecadal AMOC variability in the NCEP climate forecast system. *Climate Dynamics* **39**:3-4, 531-555. [CrossRef]

72. Feili Li, Young-Heon Jo, W. Timothy Liu, Xiao-Hai Yan. 2012. A dipole pattern of the sea surface height anomaly in the North Atlantic: 1990s-2000s. *Geophysical Research Letters* **39**:15, n/a-n/a. [CrossRef]

73. Tong Wang, Mingcai Zhang, Qihao Yu, Huyuan Zhang. 2012. Comparing the applications of EMD and EEMD on time–frequency analysis of seismic signal. *Journal of Applied Geophysics* **83**, 29-34. [CrossRef]

74. Yih-Nen Jeng, Tzung-Ming Yang, You-Chi Cheng. 2012. A class of fast and accurate deterministic trend decomposition in the spectral domain using simple and sharp diffusive filters. *Journal of the Franklin Institute* **349**:6, 2065-2092. [CrossRef]

75. Chenxing Wang, Feipeng Da. 2012. Phase demodulation using adaptive windowed Fourier transform based on Hilbert-Huang transform. *Optics Express* **20**:16, 18459. [CrossRef]

76. Jiangjiang Xia, Zhongwei Yan, Peili Wu. 2012. Multidecadal variability in local growing season during 1901–2009. *Climate Dynamics* . [CrossRef]

77. Xiyuan Hu, Silong Peng, Wen-Liang Hwang. 2012. Multicomponent AM-FM signal separation and demodulation with null space pursuit. *Signal, Image and Video Processing* . [CrossRef]

78. PETER C. CHU, CHENWU FAN, NORDEN HUANG. 2012. COMPACT EMPIRICAL MODE DECOMPOSITION: AN ALGORITHM TO REDUCE MODE MIXING, END EFFECT, AND DETREND UNCERTAINTY. *Advances in Adaptive Data Analysis* **04**:03. . [Citation] [PDF Plus]

79. XIYUAN HU, SILONG PENG, JIE TAN, WEIPING HU. 2012. BACK PROJECTION STRATEGY FOR SOLVING MODE MIXING PROBLEM. *International Journal of Wavelets, Multiresolution and Information Processing* **10**:04. . [Abstract] [References] [PDF] [PDF Plus]

80. Guojun Li, Xiaopin Zeng, Xiaona Zhou, Yu Zhou, Guojin Liu, Xichuan Zhou. 2012. Robust suppression of nonstationary power-line interference in electrocardiogram signals. *Physiological Measurement* **33**:7, 1151-1169. [CrossRef]

81. T.Y. Wu, J.C. Chen, C.C. Wang. 2012. Characterization of gear faults in variable rotating speed using Hilbert-Huang Transform and instantaneous dimensionless frequency normalization. *Mechanical Systems and Signal Processing* **30**, 103-122. [CrossRef]

82. Omid Bahar, Soheil Ramezani. 2012. Enhanced Hilbert-Huang transform and its application to modal identification. *The Structural Design of Tall and Special Buildings* n/a-n/a. [CrossRef]

83. Vasileios S. Charisis, Leontios J. Hadjileontiadis, Christos N. Liatsos, Christos C. Mavrogiannis, George D. Sergiadis. 2012. Capsule endoscopy image analysis using texture information from various colour models. *Computer Methods and Programs in Biomedicine* **107**:1, 61-74. [CrossRef]

84. Wei Guo, Peter W. Tse, Alexandar Djordjevich. 2012. Faulty bearing signal recovery from large noise using a hybrid method based on spectral kurtosis and ensemble empirical mode decomposition. *Measurement* **45**:5, 1308-1322. [CrossRef]

85. Christian Franzke. 2012. Nonlinear Trends, Long-Range Dependence, and Climate Noise Properties of Surface Temperature. *Journal of Climate* **25**:12, 4172-4183. [CrossRef]

86. Xiang Zhou, Tao Yang, Haihua Zou, Hong Zhao. 2012. Multivariate empirical mode decomposition approach for adaptive denoising of fringe patterns. *Optics Letters* **37**:11, 1904. [CrossRef]

87. Haibin Song, Yang Bai, Luis Pinheiro, Chongzhi Dong, Xinghui Huang, Boran Liu. 2012. Analysis of ocean internal waves imaged by multichannel reflection seismics, using ensemble empirical mode decomposition. *Journal of Geophysics and Engineering* **9**:3, 302-311. [CrossRef]

88. Qi Shu, Fangli Qiao, Zhenya Song, Chunzai Wang. 2012. Sea ice trends in the Antarctic and their relationship to surface air temperature during 1979–2009. *Climate Dynamics* **38**:11-12, 2355-2363. [CrossRef]

89. James E. Overland, Muyin Wang, Kevin R. Wood, Donald B. Percival, Nicholas A. Bond. 2012. Recent Bering Sea warm and cold events in a 95-year context. *Deep Sea Research Part II: Topical Studies in Oceanography* **65-70**, 6-13. [CrossRef]

90. Y.B. Yang, C.T. Chen, K.C. Chang. 2012. On applicability of Hilbert–Huang transform for vibration analysis of a two-member truss. *The IES Journal Part A: Civil & Structural Engineering* **5**:2, 67-78. [CrossRef]

91. V. Misra, J.-P. Michael, R. Boyles, E. P. Chassignet, M. Griffin, J. J. O'Brien. 2012. Reconciling the Spatial Distribution of the Surface Temperature Trends in the Southeastern United States. *Journal of Climate* **25**:10, 3610-3618. [CrossRef]

92. Jieshun Zhu, Bohua Huang, Zhaohua Wu. 2012. The Role of Ocean Dynamics in the Interaction between the Atlantic Meridional and Equatorial Modes. *Journal of Climate* **25**:10, 3583-3598. [CrossRef]

93. ZHIYUAN SHEN, NAIZHANG FENG, YI SHEN. 2012. RIDGE REGRESSION MODEL-BASED ENSEMBLE EMPIRICAL MODE DECOMPOSITION FOR ULTRASOUND CLUTTER REJECTION. *Advances in Adaptive Data Analysis* **04**:01n02. . [Citation] [References] [PDF Plus]

94. V. CAPPARELLI, A. VECCHIO, V. CARBONE. 2012. EMPIRICAL MODE DECOMPOSITION DETECTS A PHASE-SHIFT OF SEASONAL OSCILLATION. *Advances in Adaptive Data Analysis* **04**:01n02. . [Citation] [References] [PDF Plus]

95. RUICHONG ZHANG. 2012. RE-EXAMINATION OF THICKNESS-RESONANCE- FREQUENCY FORMULA FOR STRUCTURAL INTEGRITY APPRAISAL AND DAMAGE DIAGNOSIS. *Advances in Adaptive Data Analysis* **04**:01n02. . [Citation] [References] [PDF Plus]

96. MIN ZHANG, YI SHEN. 2012. ENSEMBLE EMPIRICAL MODE DECOMPOSITION FOR HYPERSPECTRAL IMAGE CLASSIFICATION. *Advances in Adaptive Data Analysis* **04**:01n02. . [Citation] [References] [PDF Plus]

97. SHIH-LIN LIN, PI-CHENG TUNG, NORDEN E. HUANG. 2012. APPLICATION OF ICA–EEMD TO SECURE COMMUNICATIONS IN CHAOTIC SYSTEMS. *International Journal of Modern Physics C* **23**:04. . [Abstract] [References] [PDF] [PDF Plus]
98. HSIN CHU TSAI, CHUNG YUE WANG, NORDEN E. HUANG. 2012. FAST INSPECTION AND IDENTIFICATION TECHNIQUES FOR TRACK IRREGULARITIES BASED ON HHT ANALYSIS. *Advances in Adaptive Data Analysis* **04**:01n02. . [Citation] [References] [PDF Plus]
99. JOHN L. AVEN, ARNOLD J. MANDELL, RICHARD COPPOLA. 2012. USING EMPIRICAL MODE DECOMPOSITION WEIGHTING FUNCTIONALS AS TIME SERIES FILTERING COEFFICIENTS FOR PHYSIOLOGICAL RECORDINGS. *Advances in Adaptive Data Analysis* **04**:01n02. . [Citation] [References] [PDF Plus]
100. Qiang Zhu, Yansong Wang, Gongqi Shen. 2012. Research and Comparison of Time-frequency Techniques for Nonstationary Signals. *Journal of Computers* **7**:4. . [CrossRef]
101. Fabiano Bianchini Batista. 2012. One-dimensional smoothing using extreme envelope average. *Mechanical Systems and Signal Processing* **28**, 432-442. [CrossRef]
102. Yu Yang, Junsheng Cheng, Kang Zhang. 2012. An ensemble local means decomposition method and its application to local rub-impact fault diagnosis of the rotor systems. *Measurement* **45**:3, 561-570. [CrossRef]
103. Yu Wei, Mu-Chen Chen. 2012. Forecasting the short-term metro passenger flow with empirical mode decomposition and neural networks. *Transportation Research Part C: Emerging Technologies* **21**:1, 148-162. [CrossRef]
104. Taesam Lee, T. B. M. J. Ouarda. 2012. An EMD and PCA hybrid approach for separating noise from signal, and signal in climate change detection. *International Journal of Climatology* **32**:4, 624-634. [CrossRef]
105. Yang Wang, Guo-Wei Wei, Siyang Yang. 2012. Iterative Filtering Decomposition Based on Local Spectral Evolution Kernel. *Journal of Scientific Computing* **50**:3, 629-664. [CrossRef]
106. Peng-Xin Gao, Jing-Lan Xie, Hong-Fei Liang. 2012. Periodicity in the most violent solar eruptions: recent observations of coronal mass ejections and flares revisited. *Research in Astronomy and Astrophysics* **12**:3, 322-330. [CrossRef]
107. Yan-Fang Sang, Zhonggen Wang, Changming Liu. 2012. Period identification in hydrologic time series using empirical mode decomposition and maximum entropy spectral analysis. *Journal of Hydrology* **424-425**, 154-164. [CrossRef]
108. Biing T. Guan, William E. Wright, Chih-Hsin Chung, Shang-Tzen Chang. 2012. ENSO and PDO strongly influence Taiwan spruce height growth. *Forest Ecology and Management* **267**, 50-57. [CrossRef]
109. Xin Zhang, Xiuli Du, James Brownjohn. 2012. Frequency modulated empirical mode decomposition method for the identification of instantaneous modal parameters of aeroelastic systems. *Journal of Wind Engineering and Industrial Aerodynamics* **101**, 43-52. [CrossRef]

110. T. Lee, T. B. M. J. Ouarda. 2012. Stochastic simulation of nonstationary oscillation hydroclimatic processes using empirical mode decomposition. *Water Resources Research* **48**:2, n/a-n/a. [CrossRef]

111. Xu Zheng, Zhiyong Hao. 2012. Diagnosis of valve-slap of diesel engine with EEMD-EMD-AGST approach. *Transactions of Tianjin University* **18**:1, 26-32. [CrossRef]

112. Min-Hung Yeh. 2012. The complex bidimensional empirical mode decomposition. *Signal Processing* **92**:2, 523-541. [CrossRef]

113. Hong Hong, Xiao-hua Zhu, Wei-min Su, Run-tong Geng, Xin-long Wang. 2012. Detection of time varying pitch in tonal languages: an approach based on ensemble empirical mode decomposition. *Journal of Zhejiang University SCIENCE C* **13**:2, 139-145. [CrossRef]

114. Lian-Yu Lin, Men-Tzung Lo, Wen-Chu Chiang, Chen Lin, Patrick Chow-In Ko, Kuang-Hua Hsiung, Jiunn-Lee Lin, Wen-Jone Chen, Matthew Huei-Ming Ma. 2012. A new way to analyze resuscitation quality by reviewing automatic external defibrillator data. *Resuscitation* **83**:2, 171-176. [CrossRef]

115. Chenxing Wang, Feipeng Da. 2012. Phase retrieval for noisy fringe pattern by using empirical mode decomposition and Hilbert Huang transform. *Optical Engineering* **51**:6, 061306. [CrossRef]

116. Paulo Costa, João Barroso, Hugo Fernandes, Leontios J Hadjileontiadis. 2012. Using Peano–Hilbert space filling curves for fast bidimensional ensemble EMD realization. *EURASIP Journal on Advances in Signal Processing* **2012**:1, 181. [CrossRef]

117. Cheng Qian, ZhongWei Yan, CongBin Fu. 2012. Climatic changes in the Twenty-four Solar Terms during 1960–2008. *Chinese Science Bulletin* **57**:2-3, 276-286. [CrossRef]

118. R. Jurkonis, A. Janušauskas, V. Marozas, D. Jegelevičius, S. Daukantas, M. Patašius, A. Paunksnis, A. Lukoševičius. 2012. Algorithms and Results of Eye Tissues Differentiation Based on RF Ultrasound. *The Scientific World Journal* **2012**, 1-6. [CrossRef]

119. S. Krinidis, M. Krinidis, V. Chatzis. 2012. Workspace for image clustering based on empirical mode decomposition. *IET Image Processing* **6**:6, 778. [CrossRef]

120. V. KrishnamurthyExtreme Events and Trends in the Indian Summer Monsoon **196**, 153-168. [CrossRef]

121. Christian Franzke. 2012. Significant reduction of cold temperature extremes at Faraday/Vernadsky station in the Antarctic Peninsula. *International Journal of Climatology* n/a-n/a. [CrossRef]

122. Bohua Huang, Zeng-Zhen Hu, James L. Kinter, Zhaohua Wu, Arun Kumar. 2012. Connection of stratospheric QBO with global atmospheric general circulation and tropical SST. Part I: methodology and composite life cycle. *Climate Dynamics* **38**:1-2, 1-23. [CrossRef]

123. Jia-Rong Yeh, Tzu-Yu Lin, Yun Chen, Wei-Zen Sun, Maysam F. Abbod, Jiann-Shing Shieh. 2012. Investigating Properties of the Cardiovascular System Using Innovative Analysis Algorithms Based on Ensemble Empirical Mode Decomposition. *Computational and Mathematical Methods in Medicine* **2012**, 1-11. [CrossRef]

124. Donghoh Kim, Kyungmee O Kim, Hee-Seok Oh. 2012. Extending the scope of empirical mode decomposition by smoothing. *EURASIP Journal on Advances in Signal Processing* **2012**:1, 168. [CrossRef]

125. Chi-Jie Lu, Yuehjen E. Shao. 2012. Forecasting Computer Products Sales by Integrating Ensemble Empirical Mode Decomposition and Extreme Learning Machine. *Mathematical Problems in Engineering* **2012**, 1-15. [CrossRef]

126. Hai-Lin Feng, Yi-Ming Fang, Xuan-Qi Xiang, Jian Li, Guan-Hui Li. 2012. A Data-Driven Noise Reduction Method and Its Application for the Enhancement of Stress Wave Signals. *The Scientific World Journal* **2012**, 1-7. [CrossRef]

127. Chun-Yi Lin, Chung-Ru Ho, Quanan Zheng, Shih-Jen Huang, Nan-Jung Kuo. 2011. Variability of sea surface temperature and warm pool area in the South China Sea and its relationship to the western Pacific warm pool. *Journal of Oceanography* **67**:6, 719-724. [CrossRef]

128. Cheng Qian, Zhaohua Wu, Congbin Fu, Dongxiao Wang. 2011. On Changing El Niño: A View from Time-Varying Annual Cycle, Interannual Variability, and Mean State. *Journal of Climate* **24**:24, 6486-6500. [CrossRef]

129. Hsien-Tsai Wu, Chun-Ho Lee, Chin-Jung Chen, Cheuk-Kwan Sun. 2011. Penile Arterial Waveform Analyzer for Assessing Penile Vascular Function in Young Adults. *Annals of Biomedical Engineering* **39**:11, 2857-2868. [CrossRef]

130. Chin-Ping Hu, Yi Chou, Ming-Chya Wu, Ting-Chang Yang, Yi-Hao Su. 2011. TIME-FREQUENCY ANALYSIS OF THE SUPERORBITAL MODULATION OF THE X-RAY BINARY SMC X-1 USING THE HILBERT-HUANG TRANSFORM. *The Astrophysical Journal* **740**:2, 67. [CrossRef]

131. TAO XIONG, YUKUN BAO, ZHONGYI HU, RUI ZHANG, JINLONG ZHANG. 2011. HYBRID DECOMPOSITION AND ENSEMBLE FRAMEWORK FOR STOCK PRICE FORECASTING: A COMPARATIVE STUDY. *Advances in Adaptive Data Analysis* **03**:04, 447-482. [Citation] [References] [PDF Plus]

132. R. FALTERMEIER, A. ZEILER, A. M. TOMÉ, A. BRAWANSKI, E. W. LANG. 2011. WEIGHTED SLIDING EMPIRICAL MODE DECOMPOSITION. *Advances in Adaptive Data Analysis* **03**:04, 509-526. [Citation] [References] [PDF Plus]

133. DISHAN HUANG, YULIN XU. 2011. A NEW APPLICATION OF ENSEMBLE EMD AMELIORATING THE ERROR FROM INSUFFICIENT SAMPLING RATE. *Advances in Adaptive Data Analysis* **03**:04, 493-508. [Citation] [References] [PDF Plus]

134. CHUNG-YUE WANG, CHIN-KUO HUANG, CHIN-SHIAN CHEN. 2011. DAMAGE ASSESSMENT OF BEAM BY A QUASI-STATIC MOVING VEHICULAR LOAD. *Advances in Adaptive Data Analysis* **03**:04, 417-445. [Citation] [References] [PDF Plus]

135. Matej Žvokelj, Samo Zupan, Ivan Prebil. 2011. Non-linear multivariate and multiscale monitoring and signal denoising strategy using Kernel Principal Component Analysis combined with Ensemble Empirical Mode Decomposition method. *Mechanical Systems and Signal Processing* **25**:7, 2631-2653. [CrossRef]

136. Cheng Qian, Congbin Fu, Zhaohua Wu. 2011. Changes in the Amplitude of the Temperature Annual Cycle in China and Their Implication for Climate Change Research. *Journal of Climate* **24**:20, 5292-5302. [CrossRef]

137. V. Capparelli, A. Vecchio, V. Carbone. 2011. Long-range persistence of temperature records induced by long-term climatic phenomena. *Physical Review E* **84**:4. . [CrossRef]

138. S. Braun, M. Feldman. 2011. Decomposition of non-stationary signals into varying time scales: Some aspects of the EMD and HVD methods. *Mechanical Systems and Signal Processing* **25**:7, 2608-2630. [CrossRef]

139. Yi Zhou, Hongguang Li. 2011. Adaptive noise reduction method for DSPI fringes based on bi-dimensional ensemble empirical mode decomposition. *Optics Express* **19**:19, 18207. [CrossRef]

140. LI-CHUNG WU, CHIA CHUEN KAO, TAI-WEN HSU, KUO-CHING JAO, YI-FUNG WANG. 2011. ENSEMBLE EMPIRICAL MODE DECOMPOSITION ON STORM SURGE SEPARATION FROM SEA LEVEL DATA. *Coastal Engineering Journal* **53**:03, 223-243. [Abstract] [References] [PDF] [PDF Plus]

141. Meng Hu, Hualou Liang. 2011. Intrinsic mode entropy based on multivariate empirical mode decomposition and its application to neural data analysis. *Cognitive Neurodynamics* **5**:3, 277-284. [CrossRef]

142. Jiping Sun, Ming Li. 2011. Life detection and location methods using UWB impulse radar in a coal mine. *Mining Science and Technology (China)* **21**:5, 687-691. [CrossRef]

143. CongBin Fu, Cheng Qian, ZhaoHua Wu. 2011. Projection of global mean surface air temperature changes in next 40 years: Uncertainties of climate models and an alternative approach. *Science China Earth Sciences* **54**:9, 1400-1406. [CrossRef]

144. Xueli An, Dongxiang Jiang, Shaohua Li, Minghao Zhao. 2011. Application of the ensemble empirical mode decomposition and Hilbert transform to pedestal looseness study of direct-drive wind turbine. *Energy* **36**:9, 5508-5520. [CrossRef]

145. Chih-Sung Chen, Yih Jeng. 2011. Nonlinear data processing method for the signal enhancement of GPR data. *Journal of Applied Geophysics* **75**:1, 113-123. [CrossRef]

146. Jingliang Sun, Huanye Sheng. 2011. A hybrid detrending method for fractional Gaussian noise. *Physica A: Statistical Mechanics and its Applications* **390**:17, 2995-3001. [CrossRef]

147. A Stroeer, L Blackburn, J Camp. 2011. Comparison of signals from gravitational wave detectors with instantaneous time–frequency maps. *Classical and Quantum Gravity* **28**:15, 155001. [CrossRef]

148. Kang-Ming Chang, Shing-Hong Liu. 2011. Gaussian Noise Filtering from ECG by Wiener Filter and Ensemble Empirical Mode Decomposition. *Journal of Signal Processing Systems* **64**:2, 249-264. [CrossRef]

149. Zhaohua Wu, Norden E. Huang, John M. Wallace, Brian V. Smoliak, Xianyao Chen. 2011. On the time-varying trend in global-mean surface temperature. *Climate Dynamics* **37**:3-4, 759-773. [CrossRef]

150. Jinjiang Wang, Robert X Gao, Ruqiang Yan. 2011. Broken-Rotor-Bar Diagnosis for Induction Motors. *Journal of Physics: Conference Series* **305**, 012026. [CrossRef]

151. Mu-Chen Chen, Yu Wei. 2011. Exploring time variants for short-term passenger flow. *Journal of Transport Geography* **19**:4, 488-498. [CrossRef]

152. Clément Gallet, Bruno Chapuis, Christian Barrès, Claude Julien. 2011. Time–frequency analysis of the baroreflex control of renal sympathetic nerve activity in the rat. *Journal of Neuroscience Methods* **198**:2, 336-343. [CrossRef]

153. Yaguo Lei, Zhengjia He, Yanyang Zi. 2011. EEMD method and WNN for fault diagnosis of locomotive roller bearings. *Expert Systems with Applications* **38**:6, 7334-7341. [CrossRef]

154. C.-Y. Chang, J. C. H. Chiang, M. F. Wehner, A. R. Friedman, R. Ruedy. 2011. Sulfate Aerosol Control of Tropical Atlantic Climate over the Twentieth Century. *Journal of Climate* **24**:10, 2540-2555. [CrossRef]

155. Tarik Al-ani, Fanny Cazettes, Stéphane Palfi, Jean-Pascal Lefaucheur. 2011. Automatic removal of high-amplitude stimulus artefact from neuronal signal recorded in the subthalamic nucleus. *Journal of Neuroscience Methods* **198**:1, 135-146. [CrossRef]

156. Chun-Yi Lin, Chung-Ru Ho, Quanan Zheng, Nan-Jung Kuo, Ping Chang. 2011. Warm pool variability and heat flux change in the global oceans. *Global and Planetary Change* **77**:1-2, 26-33. [CrossRef]

157. ZHAOHUA WU, NORDEN E. HUANG, XIANYAO CHEN. 2011. SOME CONSIDERATIONS ON PHYSICAL ANALYSIS OF DATA. *Advances in Adaptive Data Analysis* **03**:01n02, 95-113. [Citation] [References] [PDF Plus]

158. THOMAS Y. HOU, ZUOQIANG SHI. 2011. ADAPTIVE DATA ANALYSIS VIA SPARSE TIME-FREQUENCY REPRESENTATION. *Advances in Adaptive Data Analysis* **03**:01n02, 1-28. [Citation] [References] [PDF Plus]

159. NORDEN E. HUANG, XIANYAO CHEN, MEN-TZUNG LO, ZHAOHUA WU. 2011. ON HILBERT SPECTRAL REPRESENTATION: A TRUE TIME-FREQUENCY REPRESENTATION FOR NONLINEAR AND NONSTATIONARY DATA. *Advances in Adaptive Data Analysis* **03**:01n02, 63-93. [Citation] [References] [PDF Plus]

160. Michael Feldman. 2011. Hilbert transform in vibration analysis. *Mechanical Systems and Signal Processing* **25**:3, 735-802. [CrossRef]

161. P.X. Gao, H.F. Liang, W.W. Zhu. 2011. Periodicity of flare index revisited using the Hilbert–Huang transform method. *New Astronomy* **16**:3, 147-151. [CrossRef]

162. Bradley L. Barnhart, William E. Eichinger. 2011. Analysis of Sunspot Variability Using the Hilbert–Huang Transform. *Solar Physics* **269**:2, 439-449. [CrossRef]

163. Michael FeldmanReferences 275-285. [CrossRef]

164. Cheng Qian, Zhongwei Yan, Zhaohua Wu, Congbin Fu, Kai Tu. 2011. Trends in temperature extremes in association with weather-intraseasonal fluctuations in eastern China. *Advances in Atmospheric Sciences* **28**:2, 297-309. [CrossRef]

165. Cheng Qian, Congbin Fu, Zhaohua Wu, Zhongwei Yan. 2011. The role of changes in the annual cycle in earlier onset of climatic spring in northern China. *Advances in Atmospheric Sciences* **28**:2, 284-296. [CrossRef]

166. Ingrid Daubechies, Jianfeng Lu, Hau-Tieng Wu. 2011. Synchrosqueezed wavelet transforms: An empirical mode decomposition-like tool. *Applied and Computational Harmonic Analysis* **30**:2, 243-261. [CrossRef]

167. Zhongwei Yan, Jiangjiang Xia, Cheng Qian, Wen Zhou. 2011. Changes in seasonal cycle and extremes in China during the period 1960–2008. *Advances in Atmospheric Sciences* **28**:2, 269-283. [CrossRef]

168. María Belén Bernini, Alejandro Federico, Guillermo H. Kaufmann. 2011. Phase measurement in temporal speckle pattern interferometry signals presenting low-modulated regions by means of the bidimensional empirical mode decomposition. *Applied Optics* **50**:5, 641. [CrossRef]

169. Sébastien Debert, Marc Pachebat, Vincent Valeau, Yves Gervais. 2011. Ensemble-Empirical-Mode-Decomposition method for instantaneous spatial-multi-scale decomposition of wall-pressure fluctuations under a turbulent flow. *Experiments in Fluids* **50**:2, 339-350. [CrossRef]

170. Laurence C. Breaker, Alexander Ruzmaikin. 2011. The 154-year record of sea level at San Francisco: extracting the long-term trend, recent changes, and other tidbits. *Climate Dynamics* **36**:3-4, 545-559. [CrossRef]

171. Hsien-Tsai Wu, Chun-Ho Lee, An-Bang Liu, Wei-Sheng Chung, Chieh-Ju Tang, Cheuk-Kwan Sun, Hon-Kan Yip. 2011. Arterial Stiffness Using Radial Arterial Waveforms Measured at the Wrist as an Indicator of Diabetic Control in the Elderly. *IEEE Transactions on Biomedical Engineering* **58**:2, 243-252. [CrossRef]

172. T. Lee, T. B. M. J. Ouarda. 2011. Prediction of climate nonstationary oscillation processes with empirical mode decomposition. *Journal of Geophysical Research* **116**:D6. . [CrossRef]

173. Artur P. Palacz, Huijie Xue, Carrie Armbrecht, Caiyun Zhang, Fei Chai. 2011. Seasonal and inter-annual changes in the surface chlorophyll of the South China Sea. *Journal of Geophysical Research* **116**:C9. . [CrossRef]

174. Yu Zhou, Yee Leung. 2010. Empirical mode decomposition and long-range correlation analysis of sunspot time series. *Journal of Statistical Mechanics: Theory and Experiment* **2010**:12, P12006. [CrossRef]

175. A. Vecchio, V. Carbone. 2010. Amplitude-frequency fluctuations of the seasonal cycle, temperature anomalies, and long-range persistence of climate records. *Physical Review E* **82**:6. . [CrossRef]

176. Y. S. Lee, A. F. Vakakis, D. M. McFarland, L. A. Bergman. 2010. A global-local approach to nonlinear system identification: A review. *Structural Control and Health Monitoring* **17**:7, 742-760. [CrossRef]

177. Dan Chen, Duan Li, Muzhou Xiong, Hong Bao, Xiaoli Li. 2010. GPGPU-Aided Ensemble Empirical-Mode Decomposition for EEG Analysis During Anesthesia. *IEEE Transactions on Information Technology in Biomedicine* **14**:6, 1417-1427. [CrossRef]

178. Christian Franzke. 2010. Long-Range Dependence and Climate Noise Characteristics of Antarctic Temperature Data. *Journal of Climate* **23**:22, 6074-6081. [CrossRef]

179. Oumar Niang, Éric Delechelle, Jacques Lemoine. 2010. A Spectral Approach for Sifting Process in Empirical Mode Decomposition. *IEEE Transactions on Signal Processing* **58**:11, 5612-5623. [CrossRef]

180. YU-MEI CHANG, ZHAOHUA WU, JULIUS CHANG, NORDEN E. HUANG. 2010. MODEL VALIDATION BASED ON ENSEMBLE EMPIRICAL MODE DECOMPOSITION. *Advances in Adaptive Data Analysis* **02**:04, 415-428. [Citation] [References] [PDF Plus]

181. ZHAOHUA WU, NORDEN E. HUANG. 2010. ON THE FILTERING PROPERTIES OF THE EMPIRICAL MODE DECOMPOSITION. *Advances in Adaptive Data Analysis* **02**:04, 397-414. [Citation] [References] [PDF Plus]

182. T. YAN, L. J. PIETRAFESA, D. A. DICKEY, S. BAO, N. E. HUANG, Z. WU. 2010. NORTH ATLANTIC OCEAN BASIN TROPICAL CYCLONE ACTIVITY AS RELATED TO CLIMATE FACTORS FOR THE 2010 HURRICANE SEASON. *Advances in Adaptive Data Analysis* **02**:04, 463-508. [Citation] [References] [PDF Plus]

183. SUN-HUA PAO, CHIEH-NENG YOUNG, CHIEN-LUN TSENG, NORDEN E. HUANG. 2010. SMOOTHING EMPIRICAL MODE DECOMPOSITION: A PATCH TO IMPROVE THE DECOMPOSED ACCURACY. *Advances in Adaptive Data Analysis* **02**:04, 521-543. [Citation] [References] [PDF Plus]

184. Hong Hong, Zhengmin Zhao, Xinlong Wang, Zhiyong Tao. 2010. Detection of Dynamic Structures of Speech Fundamental Frequency in Tonal Languages. *IEEE Signal Processing Letters* **17**:10, 843-846. [CrossRef]

185. Jian Zhang, Ruqiang Yan, Robert X. Gao, Zhihua Feng. 2010. Performance enhancement of ensemble empirical mode decomposition. *Mechanical Systems and Signal Processing* **24**:7, 2104-2123. [CrossRef]

186. Fei Bao, Xinlong Wang, Zhiyong Tao, Qingfu Wang, Shuanping Du. 2010. EMD-based extraction of modulated cavitation noise. *Mechanical Systems and Signal Processing* **24**:7, 2124-2136. [CrossRef]

187. S. Tsakirtzis, Y.S. Lee, A.F. Vakakis, L.A. Bergman, D.M. McFarland. 2010. Modelling of nonlinear modal interactions in the transient dynamics of an elastic rod with an essentially nonlinear attachment. *Communications in Nonlinear Science and Numerical Simulation* **15**:9, 2617-2633. [CrossRef]

188. Cheng Qian, Zhaohua Wu, Congbin Fu, Tianjun Zhou. 2010. On multi-timescale variability of temperature in China in modulated annual cycle reference frame. *Advances in Atmospheric Sciences* **27**:5, 1169-1182. [CrossRef]

189. Bogdan Mijović, M De Vos, I Gligorijević, J Taelman, S Van Huffel. 2010. Source Separation From Single-Channel Recordings by Combining Empirical-Mode Decomposition and Independent Component Analysis. *IEEE Transactions on Biomedical Engineering* **57**:9, 2188-2196. [CrossRef]

190. DANIEL N. KASLOVSKY, FRANÇOIS G. MEYER. 2010. NOISE CORRUPTION OF EMPIRICAL MODE DECOMPOSITION AND ITS EFFECT ON INSTANTANEOUS FREQUENCY. *Advances in Adaptive Data Analysis* **02**:03, 373-396. [Citation] [References] [PDF Plus]

191. GANG WANG, XIAN-YAO CHEN, FANG-LI QIAO, ZHAOHUA WU, NORDEN E. HUANG. 2010. ON INTRINSIC MODE FUNCTION. *Advances in Adaptive Data Analysis* **02**:03, 277-293. [Citation] [References] [PDF Plus]

192. Ming-Juin Lin, Yih Jeng. 2010. Application of the VLF-EM method with EEMD to the study of a mud volcano in southern Taiwan. *Geomorphology* **119**:1-2, 97-110. [CrossRef]

193. J. S. F. Botha, C. Scheffer, W. W. Lubbe, A. F. Doubell. 2010. Autonomous auscultation of the human heart employing a precordial electro-phonocardiogram and ensemble empirical mode decomposition. *Australasian Physical & Engineering Sciences in Medicine* **33**:2, 171-183. [CrossRef]

194. Silong Peng, Wen-Liang Hwang. 2010. Null Space Pursuit: An Operator-based Approach to Adaptive Signal Separation. *IEEE Transactions on Signal Processing* **58**:5, 2475-2483. [CrossRef]

195. Matej Žvokelj, Samo Zupan, Ivan Prebil. 2010. Multivariate and multiscale monitoring of large-size low-speed bearings using Ensemble Empirical Mode Decomposition method combined with Principal Component Analysis. *Mechanical Systems and Signal Processing* **24**:4, 1049-1067. [CrossRef]

196. Fu Mao-Jing, Zhuang Jian-Jun, Hou Feng-Zhen, Zhan Qing-Bo, Shao Yi, Ning Xin-Bao. 2010. A method for extracting human gait series from accelerometer signals based on the ensemble empirical mode decomposition. *Chinese Physics B* **19**:5, 058701. [CrossRef]

197. XIANYAO CHEN, ZHAOHUA WU, NORDEN E. HUANG. 2010. THE TIME-DEPENDENT INTRINSIC CORRELATION BASED ON THE EMPIRICAL MODE DECOMPOSITION. *Advances in Adaptive Data Analysis* **02**:02, 233-265. [Citation] [References] [PDF Plus]

198. JIA-RONG YEH, JIANN-SHING SHIEH, NORDEN E. HUANG. 2010. COMPLEMENTARY ENSEMBLE EMPIRICAL MODE DECOMPOSITION: A NOVEL NOISE ENHANCED DATA ANALYSIS METHOD. *Advances in Adaptive Data Analysis* **02**:02, 135-156. [Citation] [References] [PDF Plus]

199. QIN WU, SHERMAN D. RIEMENSCHNEIDER. 2010. BOUNDARY EXTENSION AND STOP CRITERIA FOR EMPIRICAL MODE DECOMPOSITION. *Advances in Adaptive Data Analysis* **02**:02, 157-169. [Citation] [References] [PDF Plus]

200. Jun Chen, Xiaodong Shang, Xudong ZhaoGPS Multipath Effect Mitigation Algorithm Based on Empirical Mode Decomposition 2395-2404. [CrossRef]

201. N. ur Rehman, D.P. Mandic. 2010. Empirical Mode Decomposition for Trivariate Signals. *IEEE Transactions on Signal Processing* **58**:3, 1059-1068. [CrossRef]

202. Claire Vincent, Gregor Giebel, Pierre Pinson, Henrik Madsen. 2010. Resolving Nonstationary Spectral Information in Wind Speed Time Series Using the Hilbert–Huang Transform. *Journal of Applied Meteorology and Climatology* **49**:2, 253-267. [CrossRef]

203. PO-HSIANG TSUI, CHIEN-CHENG CHANG, NORDEN E. HUANG. 2010. NOISE-MODULATED EMPIRICAL MODE DECOMPOSITION. *Advances in Adaptive Data Analysis* **02**:01, 25-37. [Citation] [References] [PDF Plus]

204. Claire L. Vincent, Pierre Pinson, Gregor Giebela. 2010. Wind fluctuations over the North Sea. *International Journal of Climatology* n/a-n/a. [CrossRef]

205. Kang-Ming Chang. 2010. Ensemble empirical mode decomposition for high frequency ECG noise reduction. *Biomedizinische Technik/Biomedical Engineering* **55**:4, 193-201. [CrossRef]

206. Y Lei, M J Zuo, M Hoseini. 2010. The use of ensemble empirical mode decomposition to improve bispectral analysis for fault detection in rotating machinery. *Proceedings of the Institution of Mechanical Engineers, Part C: Journal of Mechanical Engineering Science* **224**:8, 1759-1769. [CrossRef]

207. T. Y. Wu, Y. L. Chung, C. H. Liu. 2010. Looseness Diagnosis of Rotating Machinery Via Vibration Analysis Through Hilbert–Huang Transform Approach. *Journal of Vibration and Acoustics* **132**:3, 031005. [CrossRef]

208. Fei Bao, Chen Li, Xinlong Wang, Qingfu Wang, Shuanping Du. 2010. Ship classification using nonlinear features of radiated sound: An approach based on empirical mode decomposition. *The Journal of the Acoustical Society of America* **128**:1, 206. [CrossRef]

209. Young S. Lee, Stylianos Tsakirtzis, Alexander F. Vakakis, Lawrence A. Bergman, D. Michael McFarland. 2009. Physics-Based Foundation for Empirical Mode Decomposition. *AIAA Journal* **47**:12, 2938-2963. [CrossRef]

210. Yaguo Lei, Ming J Zuo. 2009. Fault diagnosis of rotating machinery using an improved HHT based on EEMD and sensitive IMFs. *Measurement Science and Technology* **20**:12, 125701. [CrossRef]

211. GASTÓN SCHLOTTHAUER, MARÍA EUGENIA TORRES, HUGO L. RUFINER, PATRICK FLANDRIN. 2009. EMD OF GAUSSIAN WHITE NOISE: EFFECTS OF SIGNAL LENGTH AND SIFTING NUMBER ON THE STATISTICAL PROPERTIES OF INTRINSIC MODE FUNCTIONS. *Advances in Adaptive Data Analysis* **01**:04, 517-527. [Citation] [References] [PDF Plus]

212. JORDAN CAMP, ALEXANDER STROEER, JOHN CANNIZZO, ROBERT SCHOFIELD. 2009. SEARCHING FOR GRAVITATIONAL WAVES WITH THE HILBERT–HUANG TRANSFORM. *Advances in Adaptive Data Analysis* **01**:04, 643-666. [Citation] [References] [PDF Plus]

213. THOMAS Y. HOU, MIKE P. YAN, ZHAOHUA WU. 2009. A VARIANT OF THE EMD METHOD FOR MULTI-SCALE DATA. *Advances in Adaptive Data Analysis* **01**:04, 483-516. [Citation] [References] [PDF Plus]

214. ALEXANDER RUZMAIKIN, JOAN FEYNMAN. 2009. SEARCH FOR CLIMATE TRENDS IN SATELLITE DATA. *Advances in Adaptive Data Analysis* **01**:04, 667-679. [Citation] [References] [PDF Plus]

215. JUN CHEN. 2009. APPLICATION OF EMPIRICAL MODE DECOMPOSITION IN STRUCTURAL HEALTH MONITORING: SOME EXPERIENCE. *Advances in Adaptive Data Analysis* **01**:04, 601-621. [Citation] [References] [PDF Plus]

216. Michael Feldman. 2009. Analytical basics of the EMD: Two harmonics decomposition. *Mechanical Systems and Signal Processing* **23**:7, 2059-2071. [CrossRef]

217. T Y Wu, Y L Chung. 2009. Misalignment diagnosis of rotating machinery through vibration analysis via the hybrid EEMD and EMD approach. *Smart Materials and Structures* **18**:9, 095004. [CrossRef]

218. ZUORONG CHEN, ROBERT G. JEFFREY. 2009. APPLICATION OF THE EMPIRICAL MODE DECOMPOSITION TO FIELD TILTMETER DATA FOR HYDRAULIC FRACTURE MAPPING. *Advances in Adaptive Data Analysis* **01**:03, 407-424. [Citation] [References] [PDF Plus]

219. ZHAOHUA WU, NORDEN E. HUANG, XIANYAO CHEN. 2009. THE MULTI-DIMENSIONAL ENSEMBLE EMPIRICAL MODE DECOMPOSITION METHOD. *Advances in Adaptive Data Analysis* **01**:03, 339-372. [Citation] [References] [PDF Plus]

220. MEN-TZUNG LO, PING-HUANG TSAI, PEI-FENG LIN, CHEN LIN, YUE LOONG HSIN. 2009. THE NONLINEAR AND NONSTATIONARY PROPERTIES IN EEG SIGNALS: PROBING THE COMPLEX FLUCTUATIONS BY HILBERT–HUANG TRANSFORM. *Advances in Adaptive Data Analysis* **01**:03, 461-482. [Citation] [References] [PDF Plus]

221. S. BABJI, P. GORAI, A. K. TANGIRALA. 2009. DETECTION AND QUANTIFICATION OF CONTROL VALVE NONLINEARITIES USING HILBERT–HUANG TRANSFORM. *Advances in Adaptive Data Analysis* **01**:03, 425-446. [Citation] [References] [PDF Plus]

222. Men-Tzung Lo, Vera Novak, C.-K. Peng, Yanhui Liu, Kun Hu. 2009. Nonlinear phase interaction between nonstationary signals: A comparison study of methods based on Hilbert-Huang and Fourier transforms. *Physical Review E* **79**:6. . [CrossRef]

223. I Soltani Bozchalooi, Ming Liang. 2009. Parameter-free bearing fault detection based on maximum likelihood estimation and differentiation. *Measurement Science and Technology* **20**:6, 065102. [CrossRef]

224. Alexander Stroeer, John Cannizzo, Jordan Camp, Nicolas Gagarin. 2009. Methods for detection and characterization of signals in noisy data with the Hilbert-Huang transform. *Physical Review D* **79**:12. . [CrossRef]

225. Shih-Lin Lin, Pi-Cheng Tung, Norden Huang. 2009. Data analysis using a combination of independent component analysis and empirical mode decomposition. *Physical Review E* **79**:6. . [CrossRef]

226. Po-Hsiang Tsui, Chien-Cheng Chang, Chien-Chung Chang, Norden E. Huang, Ming-Chih Ho. 2009. An adaptive threshold filter for ultrasound signal rejection. *Ultrasonics* **49**:4-5, 413-418. [CrossRef]

227. Yaguo Lei, Zhengjia He, Yanyang Zi. 2009. Application of the EEMD method to rotor fault diagnosis of rotating machinery. *Mechanical Systems and Signal Processing* **23**:4, 1327-1338. [CrossRef]

228. NORDEN E. HUANG, ZHAOHUA WU, STEVEN R. LONG, KENNETH C. ARNOLD, XIANYAO CHEN, KARIN BLANK. 2009. ON INSTANTANEOUS FREQUENCY. *Advances in Adaptive Data Analysis* **01**:02, 177-229. [Citation] [References] [PDF Plus]

229. R. K. NIAZY, C. F. BECKMANN, J. M. BRADY, S. M. SMITH. 2009. PERFORMANCE EVALUATION OF ENSEMBLE EMPIRICAL MODE DECOMPOSITION. *Advances in Adaptive Data Analysis* **01**:02, 231-242. [Citation] [References] [PDF Plus]

230. Kun Hu, Men-Tzung Lo, C.K. Peng, Vera Novak, Eric A. Schmidt, Ajay Kumar, Marek Czosnyka. 2009. Nonlinear Pressure-Flow Relationship Is Able to Detect Asymmetry of Brain Blood Circulation Associated with Midline Shift. *Journal of Neurotrauma* **26**:2, 227-233. [CrossRef]

231. C.-K. PENG, MADALENA COSTA, ARY L. GOLDBERGER. 2009. ADAPTIVE DATA ANALYSIS OF COMPLEX FLUCTUATIONS IN PHYSIOLOGIC TIME SERIES. *Advances in Adaptive Data Analysis* **01**:01, 61-70. [Citation] [References] [PDF Plus]

232. Ryuho Kataoka, Yoshizumi Miyoshi, Akira Morioka. 2009. Hilbert-Huang Transform of geomagnetic pulsations at auroral expansion onset. *Journal of Geophysical Research* **114**:A9. . [CrossRef]

233. Cheng Qian, Congbin Fu, Zhaohua Wu, Zhongwei Yan. 2009. On the secular change of spring onset at Stockholm. *Geophysical Research Letters* **36**:12. . [CrossRef]